# LiDAR REMOTE SENSING

## NEZ PERCE & CLEARWATER NATIONAL FORESTS

(DELIVERY 4 – 10/24/2012)

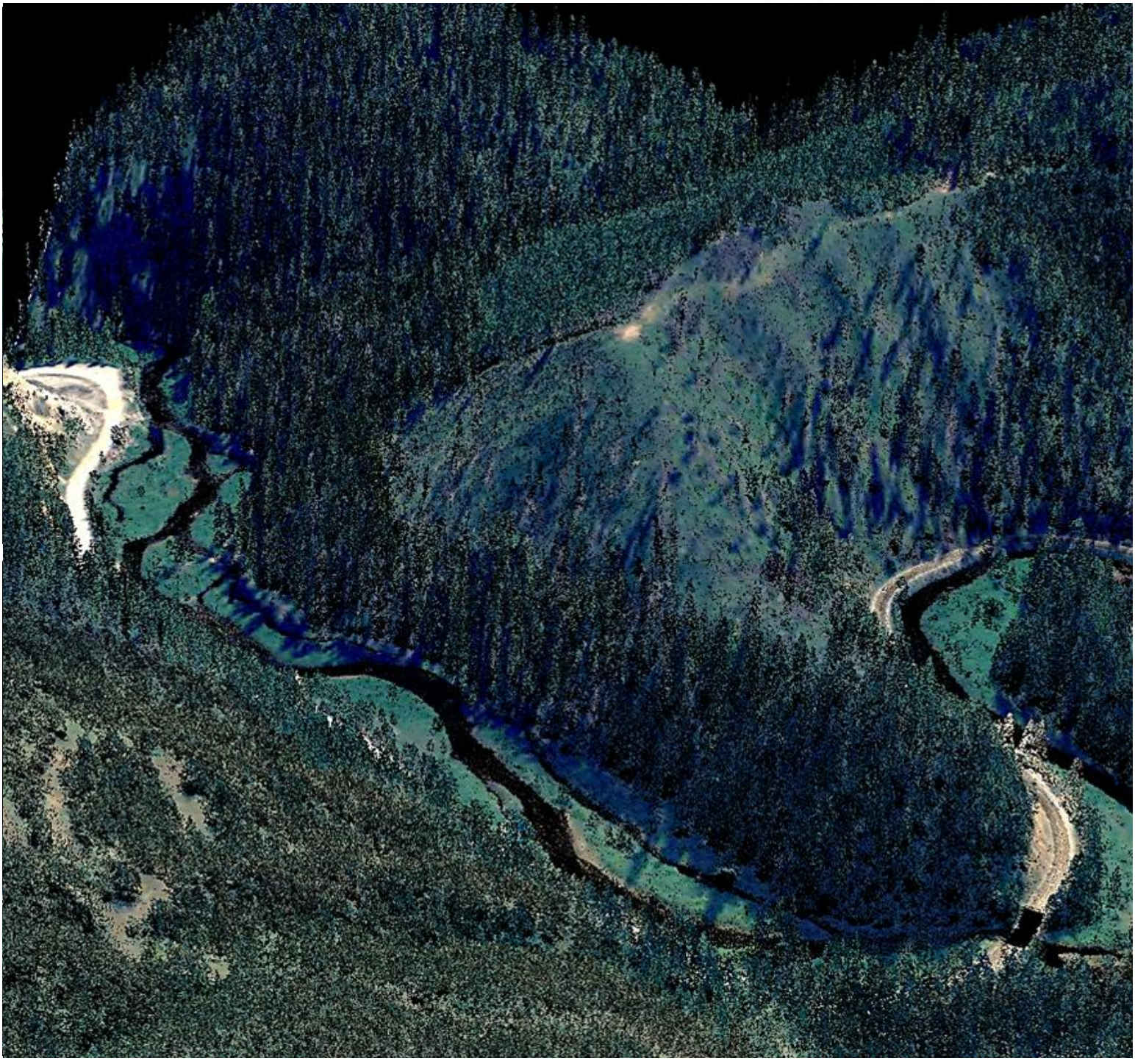


## USDA NEZ PERCE NATIONAL FOREST

**BILL CONROY** - 104 Airport Road - Grangeville, ID 83530

WSI • 517 SW 2nd Street, Suite 400 - Corvallis, OR 97333

# LiDAR Remote Sensing Data Collection: Nez Perce and Clearwater National Forests Idaho 2012

TABLE OF CONTENTS

# 1. Overview

Watershed Sciences, Inc. (WSI) has been contracted to collect Light Detection and Ranging (LiDAR) data of the within the Clearwater and Nez Perce National Forests (Figure 1). Acquisition dates, acreages, and delivery dates can be seen in Table 1. This report documents the data acquisition, processing methods, and accuracy assessment of the delivered LiDAR datasets and will be the final delivery for the project.

Figure 1. Delivery status map of the Nez Perce and Clearwater National Forests' AOIs

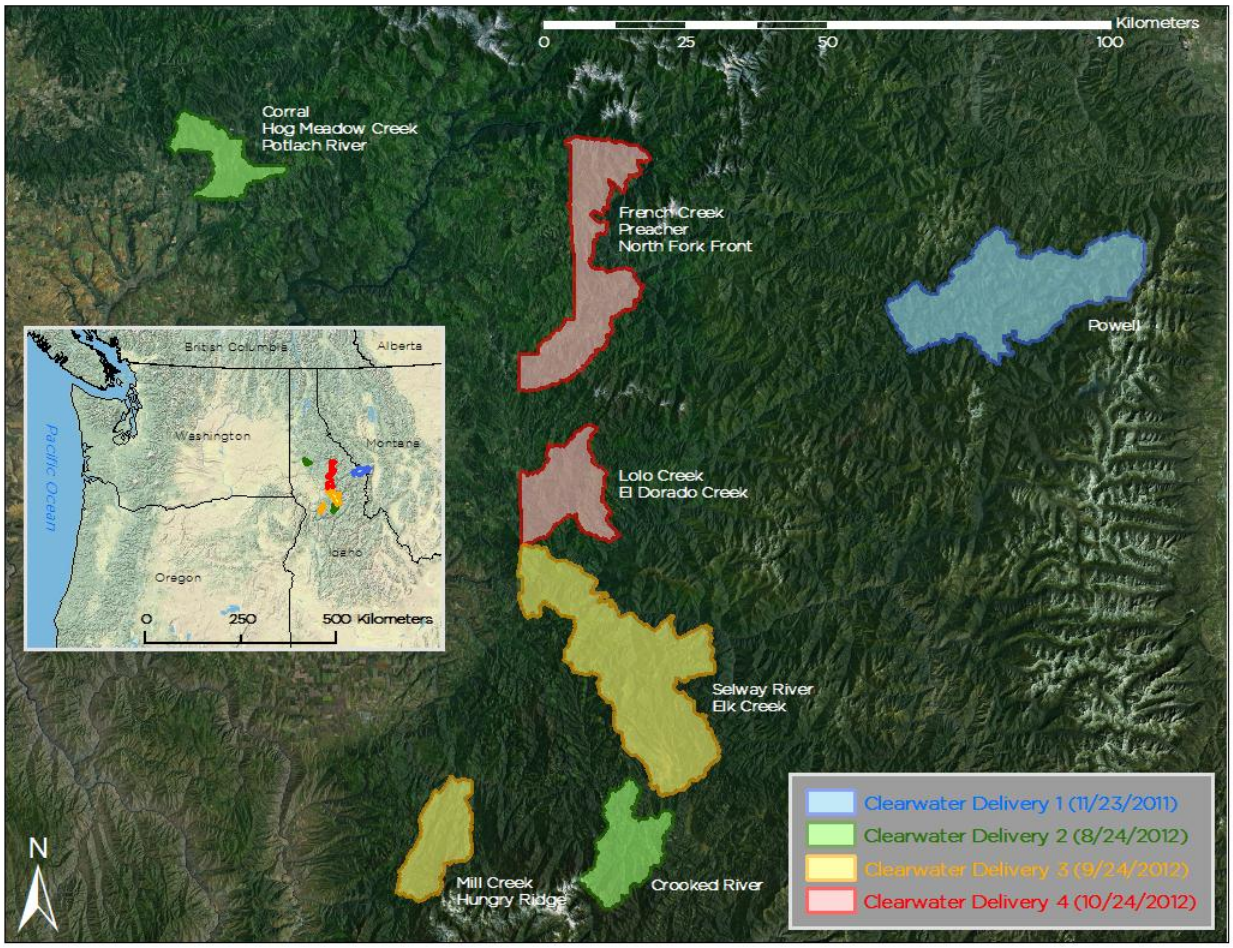

# 2. Acquisition

Table 1. Delivery status table for the Areas of Interest (AOIs) within the Nez Perce and Clearwater National Forests

| AOI | Contracted Acres | Buffered Acres | Acquisition Dates | Delivery Date |
|---|---|---|---|---|
| Powell | 132,308.3 | 136,456.7 | 9/12-14/2011<br>9/16/2011<br>9/21-23/2011 | 11/23/2011 |
| Crooked River | 45,601.1 | 47,480.4 | 7/14/2012<br>7/16-19, 2012<br>8/7/2012<br>8/11/2012 | 08/24/2012 |
| Corral Creek<br>Hog Meadow<br>Potlatch River | 32,093.4 | 33.978.5 | 5/11-13/2012 | 08/24/2012 |
| Hungry Ridge<br>Mill Creek | 39,156.9 | 40,769.9 | 7/12-13/2012<br>7/22/2012 | 09/24/2012 |
| Selway<br>Elk | 155,966.5 | 160,513.8 | 6/4/2012<br>6/7/2012<br>6/11/2012<br>6/13-16/2012<br>7/5-8/ 2012 | 09/24/2012 |
| French Preacher<br>North Fork Front | 91,943.1 | 95,799.1 | 7/9-12/2012<br>7/23-25/2012 | 10/24/2012 |
| El Dorado/ Lolo | 50,617.5 | 52,640.9 | 6/15-16/2012<br>7/4/2012 | 10/24/2012 |

## 2.1 Airborne Survey – Instrumentation and Methods

The LiDAR survey utilized two Leica ALS60 systems and one ALS50 Phase II system mounted in Cessna Caravans. The Leica systems were set to acquire ≥88,000 laser pulses per second (i.e. 88 kHz pulse rate) and flown from 1200-1300 meters above ground level (AGL) depending on weather and terrain, capturing a scan angle of ±14° from nadir. These settings were developed to yield points with an average native pulse density of ≥4 pulses per square meter over terrestrial surfaces. It is not uncommon for some types of surfaces (e.g. dense vegetation or water) to return fewer pulses than the laser originally emitted. These discrepancies between 'native' and 'delivered' density will vary depending on terrain, land cover, and the prevalence of water bodies.

All areas were surveyed with an opposing flight line side-lap of ≥50% (≥100% overlap) to reduce laser shadowing and increase surface laser painting. The Leica laser systems allow up to four range measurements (returns) per pulse, and all discernible laser returns were processed for the output dataset.

To accurately solve for laser point position (geographic coordinates x, y, z), the positional coordinates of the airborne sensor and the attitude of the aircraft were recorded continuously throughout the LiDAR data collection mission. Position of the aircraft was measured twice per second (2 Hz) by an onboard differential GPS unit. Aircraft attitude was measured 200 times per second (200 Hz) as pitch, roll, and yaw (heading) from an onboard inertial measurement unit (IMU). To allow for post-processing correction and calibration, aircraft/ sensor position and attitude data are indexed by GPS time.

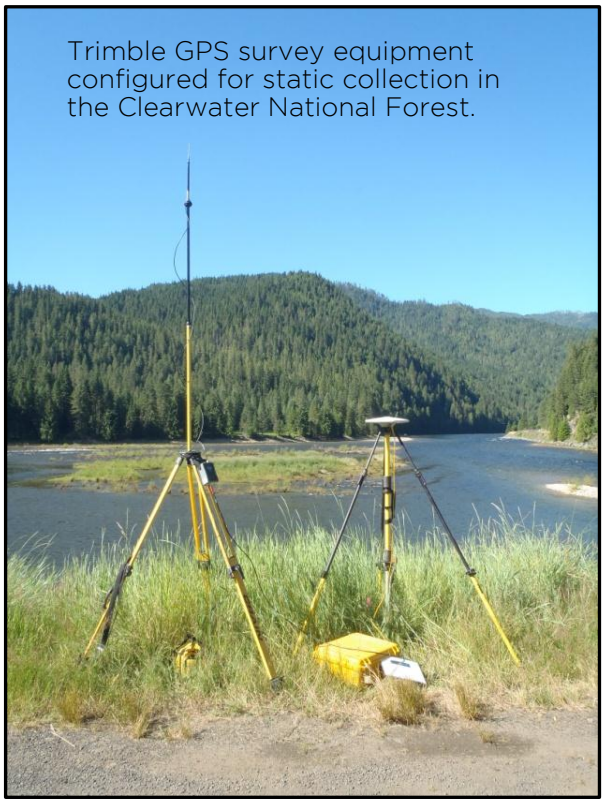

Trimble GPS survey equipment configured for static collection in the Clearwater National Forest.

## 2.2 Ground Survey - Instrumentation and Methods

All ground data (base station static and ground check points) were uploaded to company servers nightly and evaluated in the office for validity and spatial coverage. The survey control plan provided redundant control within 13 nautical miles of the mission areas for LiDAR flights. The controls were set prior to the airborne missions. Monument coordinates are provided in Table 2 and shown in Figures 2-8.

During the airborne data collection missions, WSI conducted multiple static Global Navigation Satellite System (GNSS) ground surveys (1 Hz recording frequency) over each monument. The GNSS data were used to correct the continuous onboard measurements of the aircraft position recorded throughout the mission. After the airborne survey, the static GPS data were triangulated with nearby Continuously Operating Reference Stations (CORS) using the Online Positioning User Service (OPUS[1]) for precise positioning. Multiple independent sessions over the same monument were processed to confirm antenna height measurements and refine position accuracy.

### 2.2.1 Instrumentation

All static surveys were collected either with Trimble model R7 GNSS receivers equipped with a Zephyr Geodetic Model 2 RoHS antenna (OPUS ID: TRM57971.00) or with Trimble model R8 GNSS receivers (OPUS ID: TRM_R8_GNSS). A Trimble model R8 GNSS receiver was also used for collecting check points using real time kinematic (RTK) survey techniques. All GNSS measurements are made with dual frequency L1-L2 receivers with carrier-phase correction.

### 2.2.2 Monumentation

WSI utilized 5 existing NGS monuments and established 28 new monuments, ensuring redundant ground control for LiDAR acquisition. New monumentation was set using 5/8" rebar topped with marked 2" aluminum caps. These monument locations were selected for good visibility and optimal location to provide additional RTK coverage.


[1] Online Positioning User Service (OPUS) is run by the National Geodetic Survey to process corrected monument positions.

Table 2. Base Station control coordinates for the Nez Perce and Clearwater National Forests data collection

| Base Station ID | Datum: NAD83 (CORS96) | | GRS80 |
|---|---|---|---|
| | Latitude | Longitude | Ellipsoid Z (meters) |
| AC5203 | 45°49'26.65461" | 115°26'22.56158" | 1224.552 |
| BOVL_GPS | 46°51'24.49623" | 116°24"7.29811" | 856.161 |
| CHP_01 | 46°49'28.14619" | 116°27'07.59396" | 848.350 |
| CLRWTR_01 | 46°36'14.69440" | 114°23'26.29658" | 1593.841 |
| CLRWTR_02 | 46°36'21.74383" | 114°30'45.09678" | 1568.156 |
| CLRWTR_03 | 46°30'58.12231" | 114°41'22.21175" | 1091.187 |
| CLRWTR_04 | 46°34'57.87190" | 114°36'51.27193" | 1258.272 |
| CLRWTR_05 | 46°08'34.46691" | 115°35'48.38513" | 432.354 |
| CW_CROOKED_01 | 45°44'02.48366" | 115°28'31.19473" | 1681.488 |
| CW_CROOKED_02 | 45°43'27.46270" | 115°30'24.85566" | 1659.072 |
| CW_FRENCH_01 | 46°32'26.51297" | 115°34'48.17943" | 1423.208 |
| CW_FRENCH_02 | 46°32'30.89331" | 115°35'45.12366" | 1413.962 |
| CW_FRENCH_03 | 46°41'53.08058" | 115°37'57.42855" | 1045.046 |
| CW_FRENCH_04 | 46°46°51.97256" | 115°37'03.72481" | 1534.236 |
| CW_LOLO_01 | 46°21'05.42682" | 115°41'25.23180"" | 1195.124 |
| CW_MILL_01 | 45°38'34.81785" | 116°02'00.13910" | 1635.543 |
| CW_MILL_02 | 45°42'12.09840" | 115°59'52.18188" | 1520.462 |
| CW_SELWAY_01 | 46°02'30.44178" | 115°33'32.74398" | 1454.384 |
| GRANGE_01 | 45°56'22.62025" | 116°07'26.05616" | 994.111 |
| MIDFK_1 | 45°49'12.46902" | 115°27'20.34815" | 1184.413 |
| MIDFK_2 | 45°57'56.67541" | 115°29'52.73233" | 1604.231 |
| MIDFK_3 | 45°56'37.07867" | 115°34'19.94975" | 1839.292 |
| MIDFK_4 | 46°05'28.29191" | 115°41'36.42341" | 1299.006 |
| MIDFK_5 | 46°06'39.81928" | 115°39'36.35117" | 1328.634 |
| MIDFK_6 | 46°03'23.79942" | 115°39'00.15014" | 1591.788 |
| NEZ_PERCE | 46°22'47.39583" | 117°00'42.84255" | 406.931 |
| NGS_15181 | 46°38'05.17753" | 114°34'41.07530" | 1579.596 |
| NP_CAL | 46°22'12.80069" | 117°00'56.74786" | 423.009 |
| RA1441 | 45°56'31.53290" | 116°07'09.57664" | 991.632 |
| RY0961 | 46°14'43.77270" | 115°38'03.50364" | 1575.729 |
| SELWAY_02 | 46°03'10.06652" | 115°31'57.21726" | 869.627 |
| WALDE_02 | 46°15'33.33596" | 115°46°13.81685" | 1039.884 |
| WALDE_05 | 46°14'09.96653" | 115°40'34.57233" | 1261.885 |

Figure 2. Base station and checkpoint location map for the Powell AOI

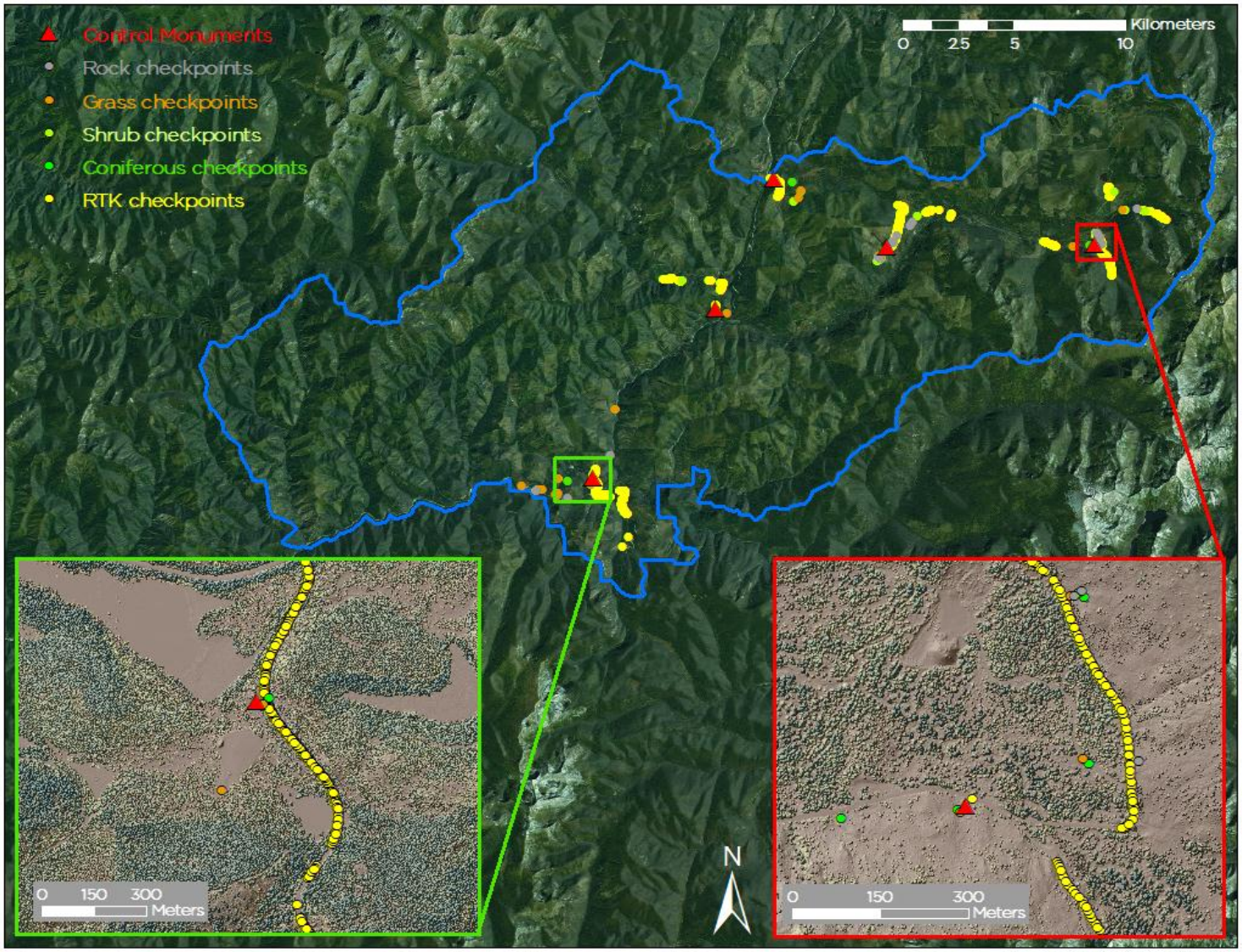

Figure 3. Base station and checkpoint location map for the Crooked River AOI

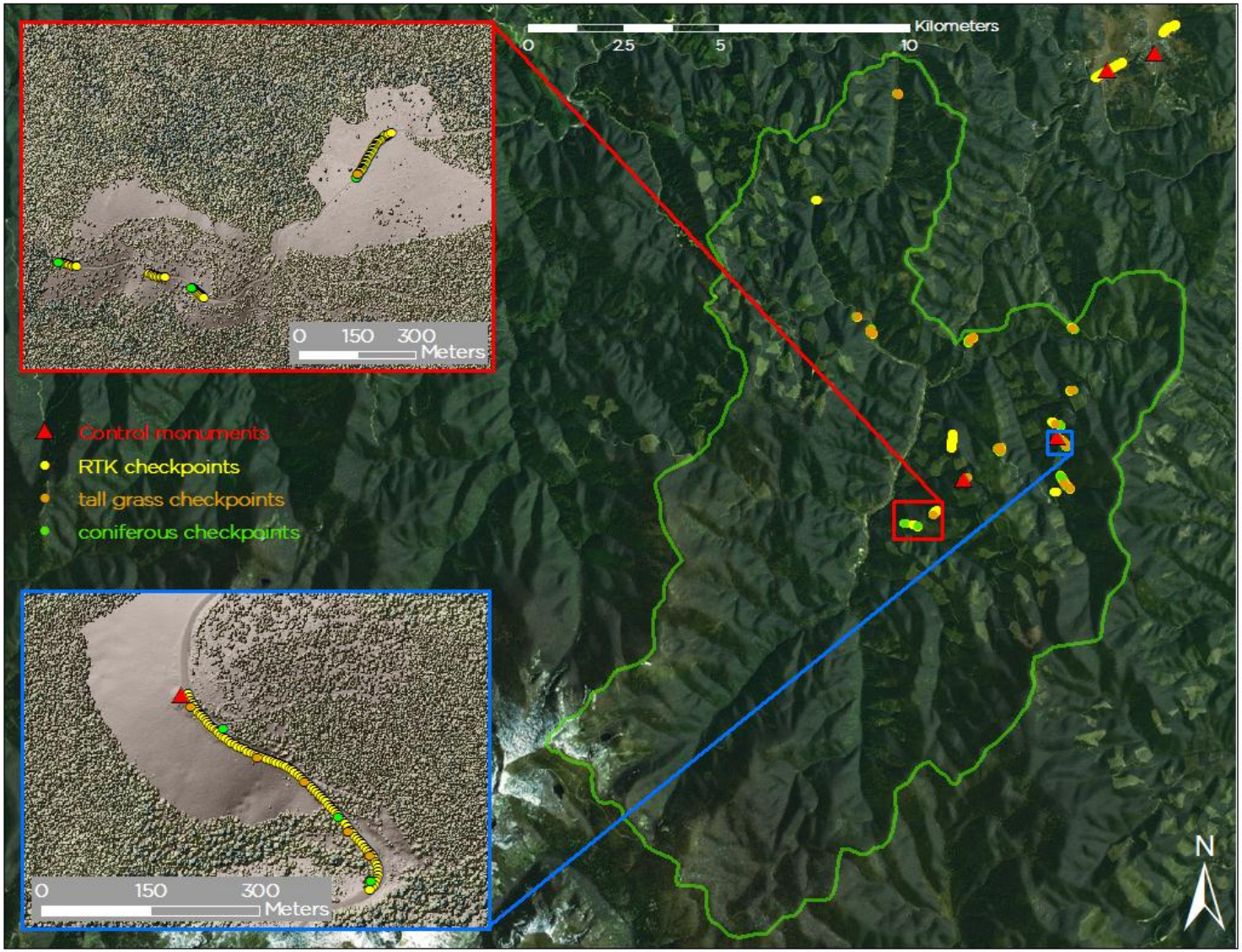

Figure 4. Base station and checkpoint location map for the Corral Creek, Hog Meadow, and Potlatch River AOI

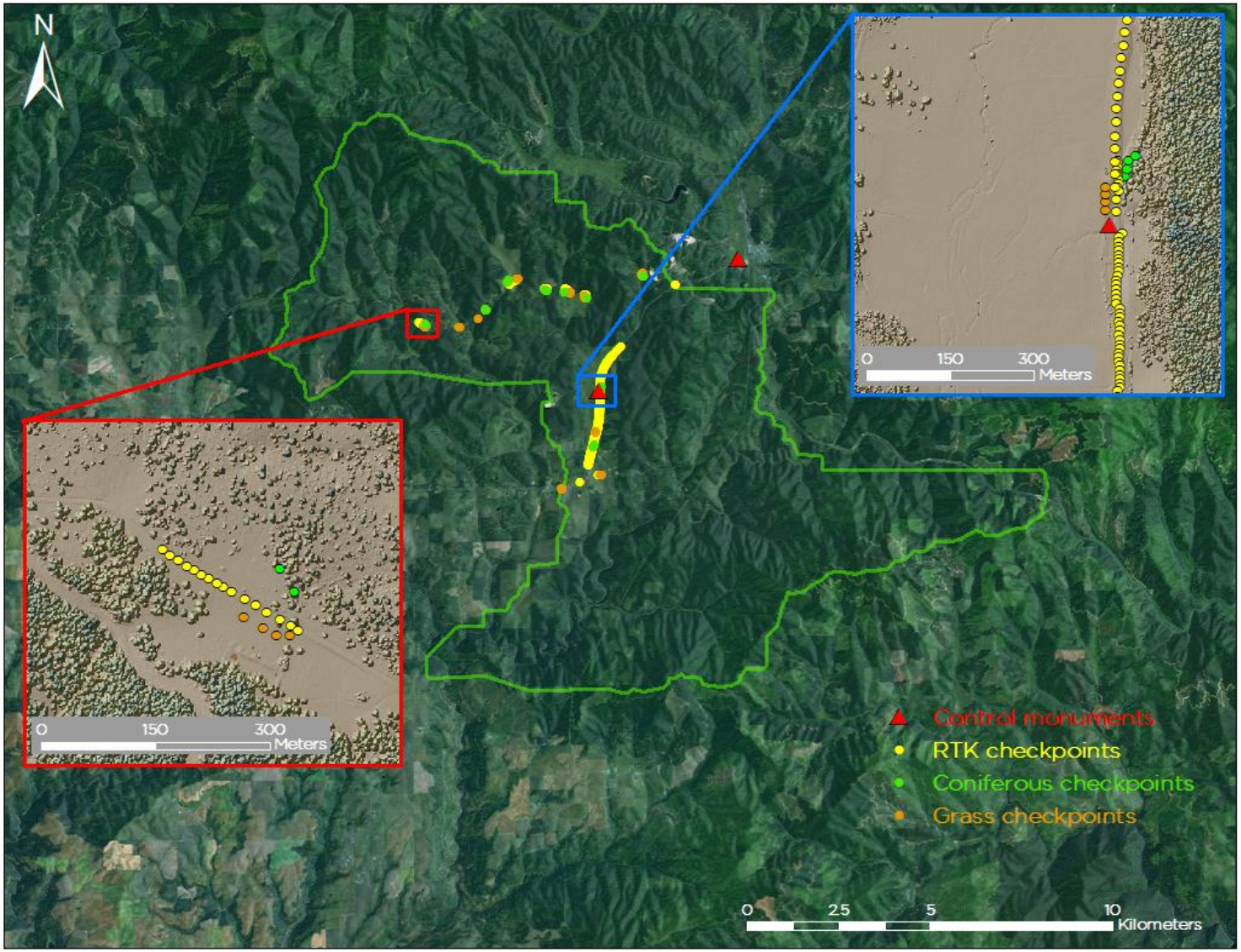

Figure 5. Base station and checkpoint location map for the Hungry Ridge and Mill Creek AOI

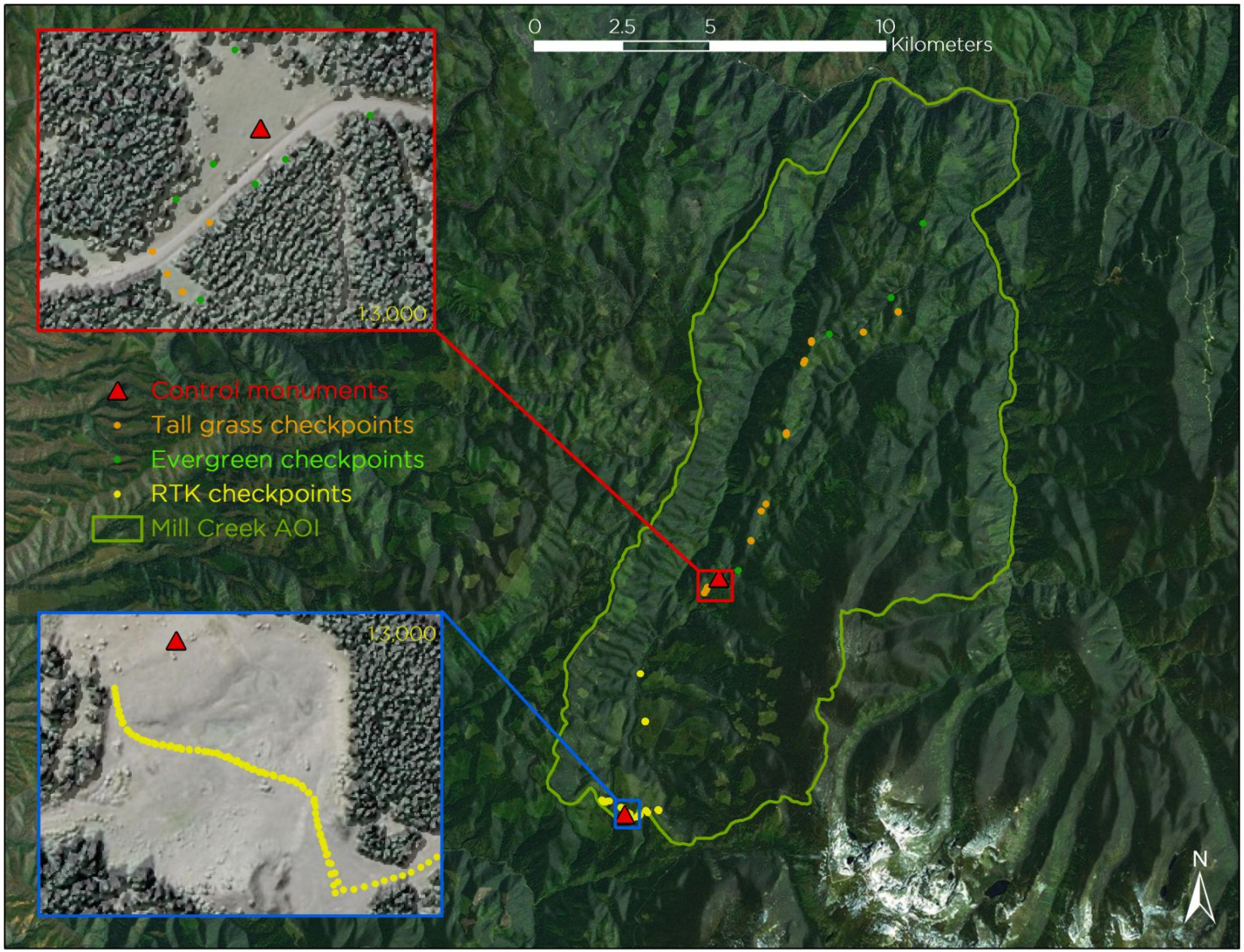

Figure 6. Base station and checkpoint location map for the Selway and Elk AOI

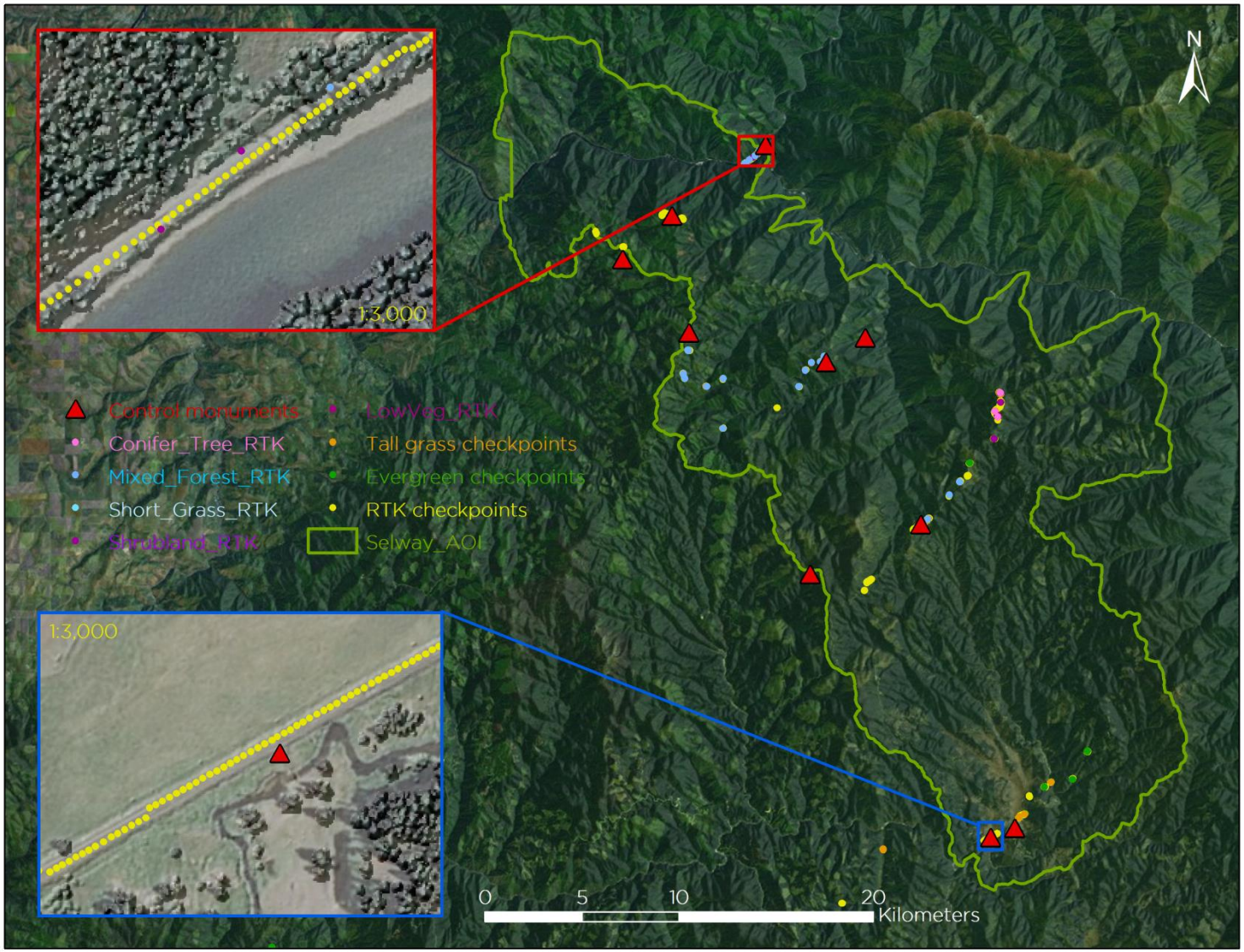

Figure 7. Base station and checkpoint location map for the French Preacher and North Fork AOI

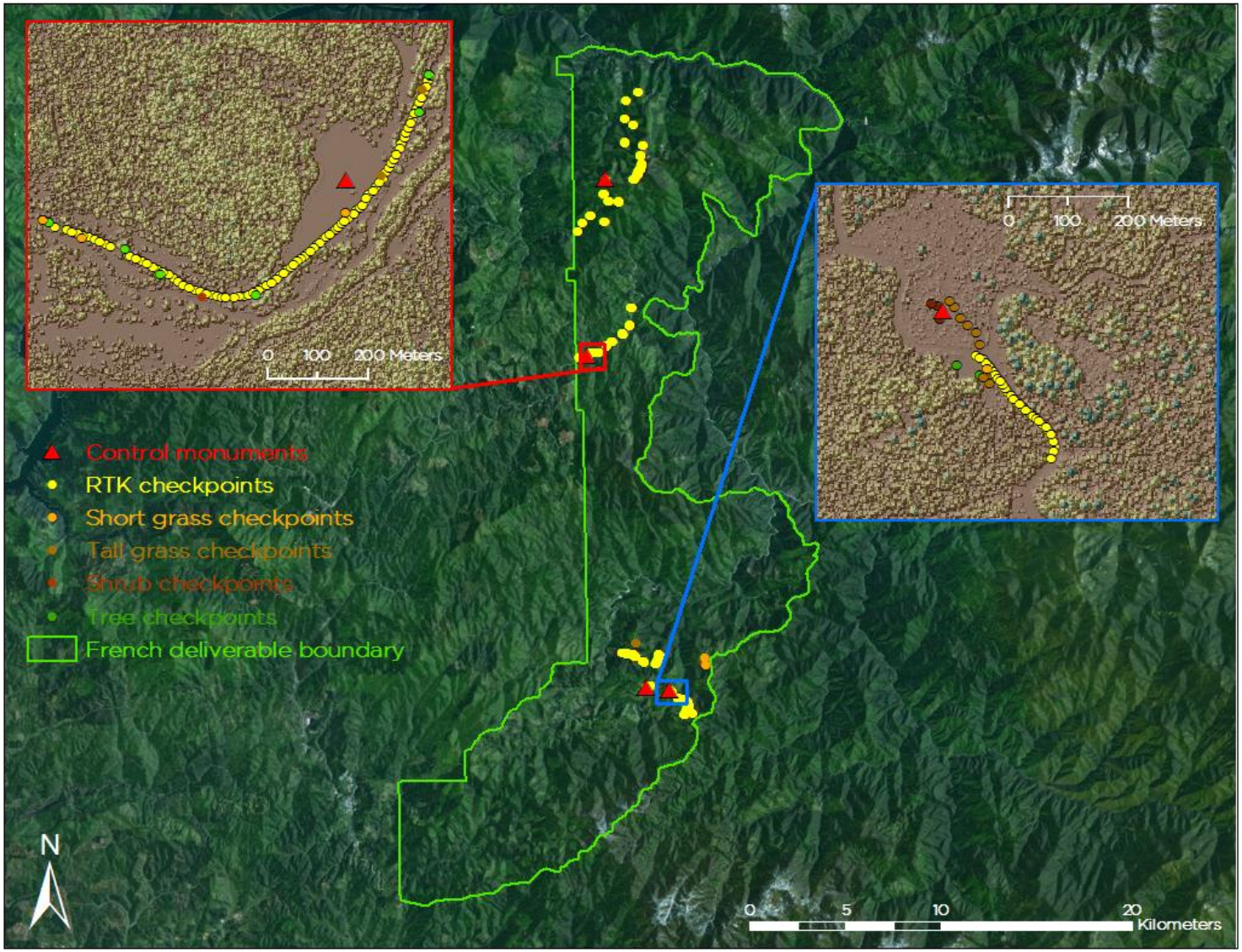

Figure 8. Base station and checkpoint location map for the El Dorado/Lolo AOI

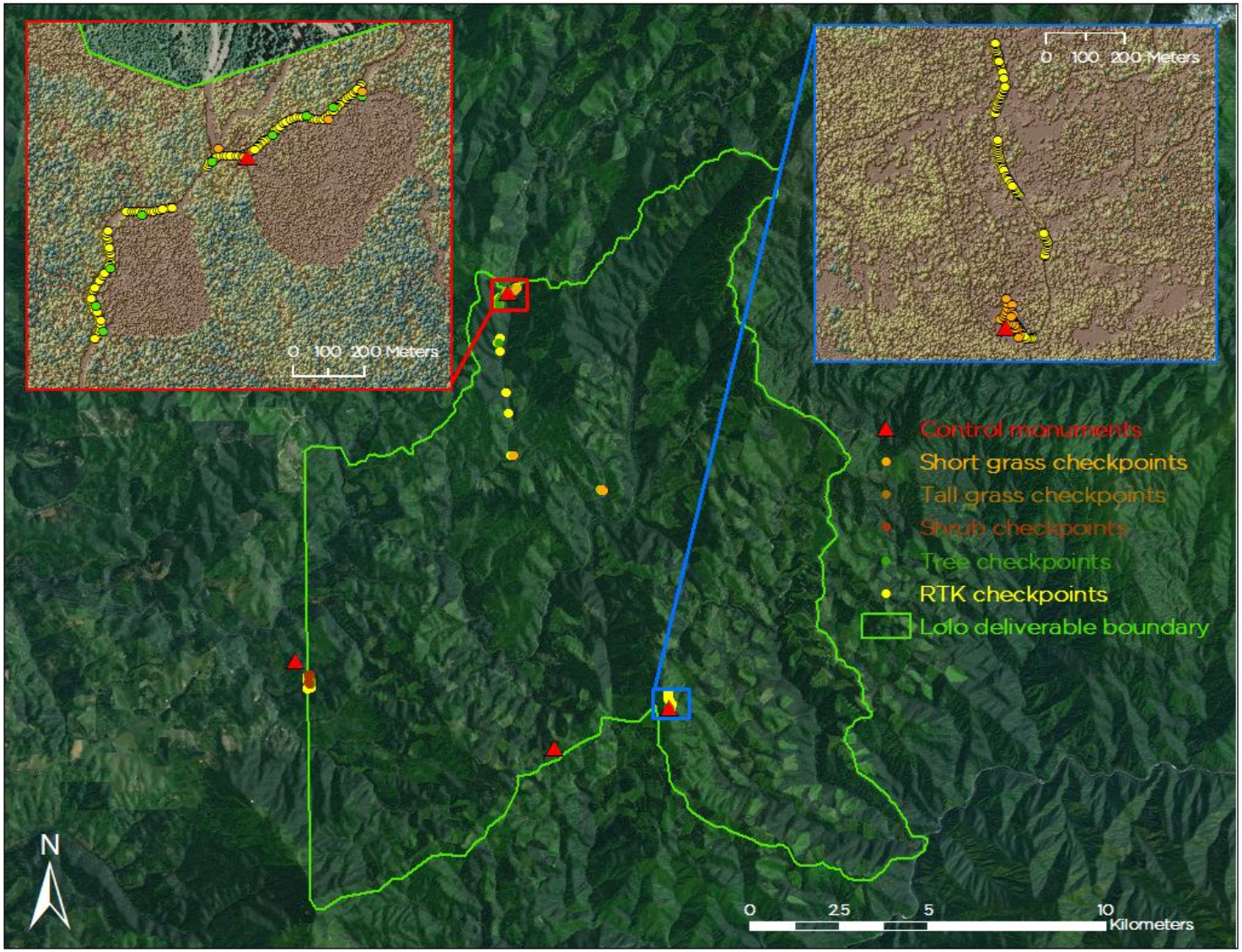

## 2.3 Methodology

All control monuments were observed for a minimum of one survey session lasting no fewer than 4 hours and another session lasting no fewer than 2 hours, resulting in two or more independent sessions to confirm monument location accuracy. Data were collected at a rate of 1Hz using a 10 degree mask on the antenna.

Monument positions were triangulated through OPUS Project using 3 or more nearby CORS stations resulting in a fully adjusted position. After multiple sessions had been collected at each monument, accuracy and error ellipses were calculated from the OPUS reports. This resulted in a rating of the monuments, based on FGDC-STD-007.2-1998[2] Part 2 Table 2.1 at the 95% confidence level. When a statistical stable position was found, CORPSCON[3] 6.0.1 and Blue Marble Desktop 2.4 software was used to convert the UTM positions to geodetic coordinates. Ground based RTK checkpoints and aircraft mounted GPS measurements were made during periods with PDOP[4] less than or equal to 3.0, with at least 6 satellites in view of both a stationary reference receiver and the roving receiver. Periods of low precision during static sessions were removed during OPUS processing. RTK positions were collected on bare earth locations such as paved or hard packed gravel roads where the ground was clearly visible (and was likely to remain visible) during the data acquisition and RTK measurement period. These checkpoints were taken no closer than one meter to any nearby terrain breaks such as road edges or drop offs.

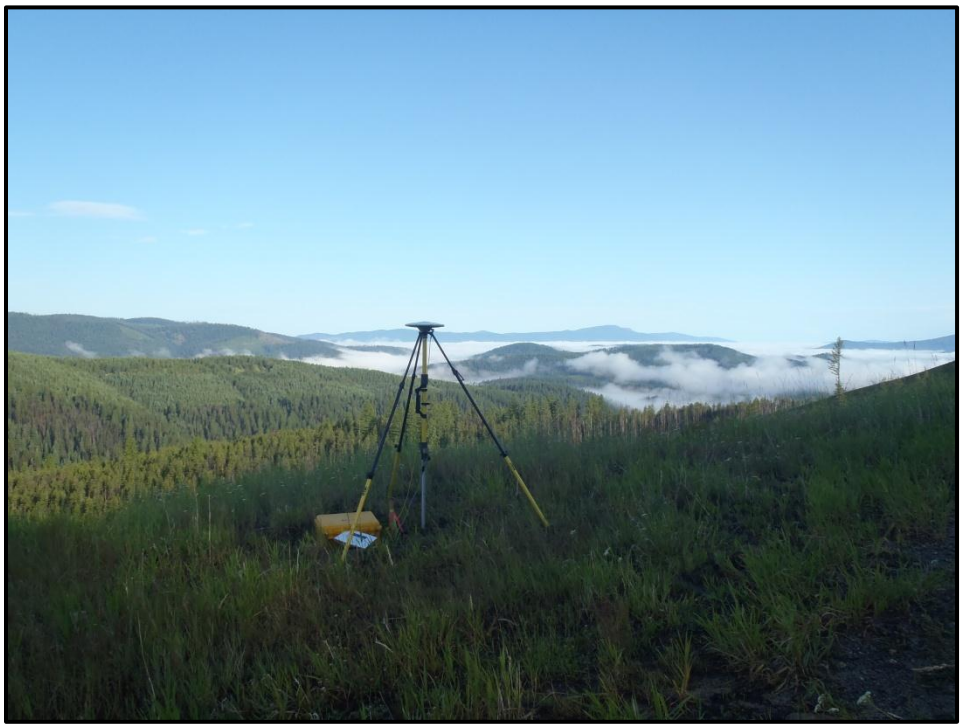

[2] Federal Geographic Data Committee Draft Geospatial Positioning Accuracy Standards
[3] U.S. Army Corps of Engineers , Army Geospatial Center software
[4]PDOP: Point Dilution of Precision is a measure of satellite geometry, the smaller the number the better the geometry between the point and the satellites.

# 3. LiDAR Data Processing

## 3.1 Applications and Work Flow Overview

1. Resolved kinematic corrections for aircraft position data using kinematic aircraft GPS and static ground GPS data.
   Software: Waypoint GPS v.8.3, Trimble Business Center v.2.72, Blue Marble Desktop v.2.4
2. Developed a smoothed best estimate of trajectory (SBET) file that blends post-processed aircraft position with attitude data. Sensor head position and attitude were calculated throughout the survey. The SBET data were used extensively for laser point processing.
   Software: IPAS TC v.3.1
3. Calculated laser point position by associating SBET position to each laser point return time, scan angle, intensity, etc. Created raw laser point cloud data for the entire survey in *.las (ASPRS v. 1.2) format. Data were converted to orthometric elevations (NAVD88) by applying a Geoid03 correction.
   Software: ALS Post Processing Software v.2.74
4. Imported raw laser points into manageable blocks (less than 500 MB) to perform manual relative accuracy calibration and filter for pits/birds. Ground points were then classified for individual flight lines (to be used for relative accuracy testing and calibration).
   Software: TerraScan v.12.004
5. Using ground classified points per each flight line, the relative accuracy was tested. Automated line-to-line calibrations were then performed for system attitude parameters (pitch, roll, heading), mirror flex (scale) and GPS/IMU drift. Calibrations were performed on ground classified points from paired flight lines. Every flight line was used for relative accuracy calibration.
   Software: TerraMatch v.12.001
6. Position and attitude data were imported. Resulting data were classified as ground and non-ground points. Statistical absolute accuracy was assessed via direct comparisons of ground classified points to ground RTK survey data.
   Software: TerraScan v.12.004, TerraModeler v.12.002
7. Bare Earth models were created as a triangulated surface and exported as ArcInfo ASCII grids at a 1-meter pixel resolution and were mosaicked as ESRI grids and ERDAS images. Vegetation canopy models were created for any class at 1-meter grid spacing and exported as ArcInfo ASCII grids and were mosaicked as ESRI grids and ERDAS images.
   Software: TerraScan v.12.004, ArcMap v. 10.0, TerraModeler v.12.002

## 3.2 Aircraft Kinematic GPS and IMU Data

Kinematic corrections for the aircraft were processed in Waypoint GPS v.8.3 and tied to the post-processed control monument locations. IPAS TC v.3.1 was used to develop a trajectory file that includes corrected aircraft position and attitude information. The trajectory data for the entire flight survey session were incorporated into a final smoothed best estimated trajectory (SBET) file that contains accurate and continuous aircraft positions and attitudes.

## 3.3 Laser Point Processing

Laser point coordinates were computed and returns (first through fourth) were assigned an associated (x, y, z) coordinate along with unique intensity values (0-255). The data were output into large LAS v. 1.2 files with each point maintaining the corresponding scan angle, return number (echo), intensity, and x, y, z (easting, northing, and elevation) information.

These initial laser point files were too large for subsequent processing. To facilitate laser point processing, a gridded tile network was created to divide the dataset into manageable sizes (< 500 MB). Laser point data were imported into the tile network using TerraScan, and manual calibration was performed to assess the system offsets for pitch, roll, heading and scale

(mirror flex). Using a geometric relationship developed by WSI, each of these offsets was resolved and corrected if necessary. LiDAR data coverage was subsequently reviewed to ensure adequate density and positional accuracy throughout the Nez Perce and Clearwater National Forests' AOIs.

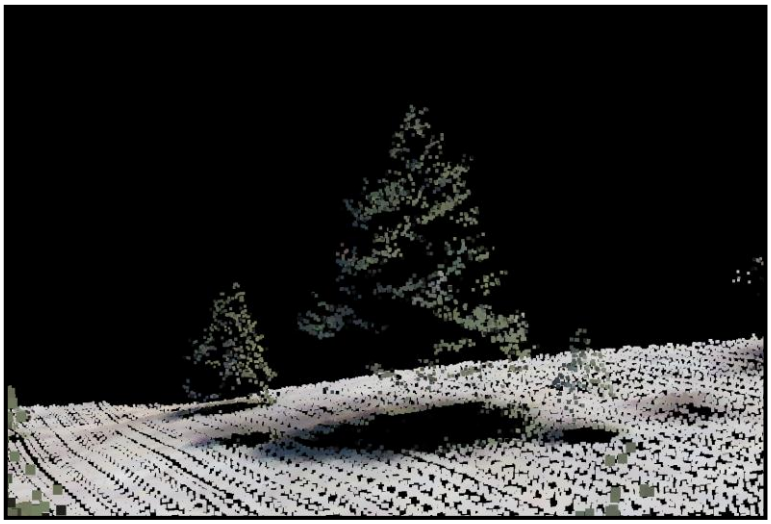

LiDAR points were then filtered for noise, pits (artificial low points), and birds (true birds as well as erroneously high points) by screening for absolute elevation limits, isolated points and height above ground. Internal calibration was subsequently refined using TerraMatch. Points from overlapping lines were tested for internal consistency and final adjustments were made for system misalignments (i.e., pitch, roll, heading offsets and scale). Automated sensor attitude and scale corrections yielded 3-5 cm improvements in the relative accuracy. Once system misalignments were corrected, vertical GPS drift was then resolved and removed per flight line, yielding a slight improvement (<1 cm) in relative accuracy.

Automated point processing was finalized using TerraScan to classify laser returns into a ground class. This is done using geometric constraints to identify near earth surface points. The resulting bare earth (ground) model was visually inspected and ground classification modifications were performed as needed to improve ground detail. This manual editing of ground often occurs in areas with known ground modeling deficiencies, such as bedrock outcrops, cliffs, deeply incised stream banks, and dense vegetation. In some cases, automated ground point classification inaccurately includes known vegetation (i.e., understory, low/dense shrubs, etc.). These points were reclassified to default. In addition, each tile was inspected for remaining pits, birds, and spurious points that were consequently removed. In a tile that contained approximately 7.5-9.0 million points, an average of 50-100 points were typically found to be artificially low or high.

# 4. LiDAR Accuracy Assessment

Laser point absolute accuracy is largely a function of laser noise and relative accuracy. To minimize these contributions to absolute error, a number of noise filtering and calibration procedures were performed (Appendix A). The LiDAR quality assurance process compares the calibrated LiDAR data to the collected RTK check points. The divergence between RTK check points and the closest ground classified LiDAR point is used to calculate absolute accuracy statistics (Section 5.4). A total of 5,390 RTK GPS measurements were collected by WSI on hard surfaces distributed among multiple flight swaths. In addition to RTK checkpoints, land cover check points were collected on various surfaces.

Statements of statistical accuracy apply to fixed terrestrial surfaces only and may not be applied to areas of dense vegetation or steep terrain.

# 5. Study Area Results

Summary statistics for accuracy (relative and absolute) and point resolution of the LiDAR data are presented below in terms of central tendency, variation around the mean, and the spatial distribution of the data (for point resolution by 100 $m^2$) (Table 3).

## 5.1 Data Summary

Table 3. LiDAR Resolution and Absolute Accuracy - Specifications and Achieved Values

| | Targeted | Achieved |
|---|---|---|
| Resolution: | ≥ 4 points/$m^2$ | 7.70 points/$m^2$ |
| Vertical Accuracy (RMSE): | <15 cm | 3.3 cm |

## 5.2 Data Density/Resolution

The average first-return density of the delivered LiDAR data is 7.70 points per square meter for the entire project area. The initial datasets, acquired to be ≥4 points per square meter, were filtered as described previously to remove spurious or inaccurate points. The pulse density distribution will vary within the study area due to laser scan pattern and flight conditions. Additionally, some types of surfaces (i.e. breaks in terrain, water, steep slopes) may return fewer pulses (delivered density) than the laser originally emitted (native density). Figures 9 and 10 show the distribution of average first return and ground point densities for each 100 $m^2$ cell. Figures 11-24 show the first return and ground density distribution maps for each AOI.

Cumulative data resolution of all AOIs for the Nez Perce and Clearwater National Forests' LiDAR data:

**Figure 9.** Nez Perce and Clearwater Forests' density distribution for first return classified laser points

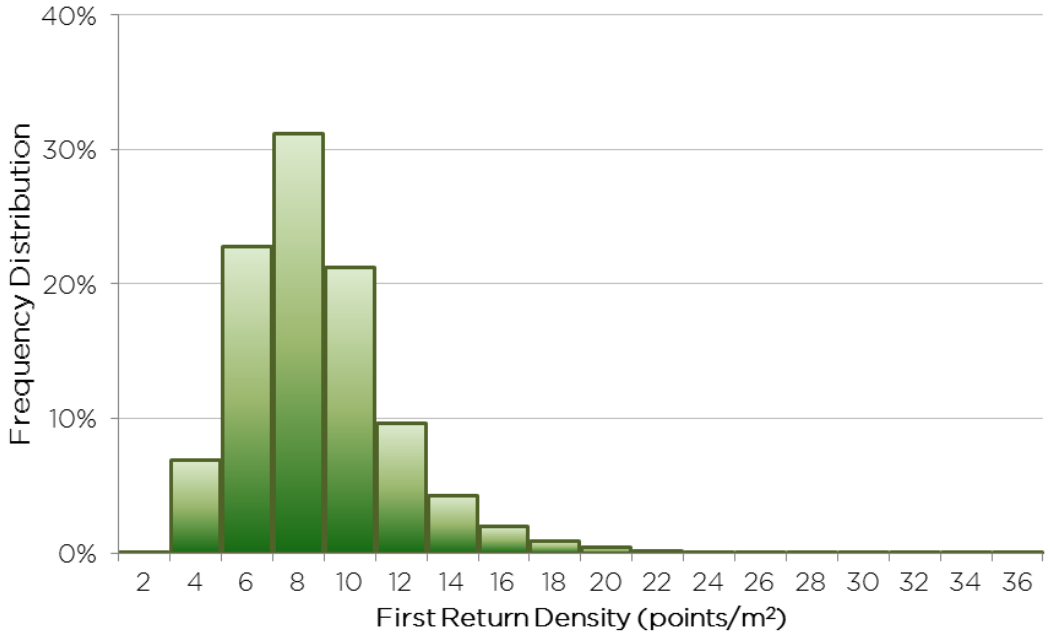


**Figure 10.** Nez Perce and Clearwater Forests' density distribution for ground classified laser points

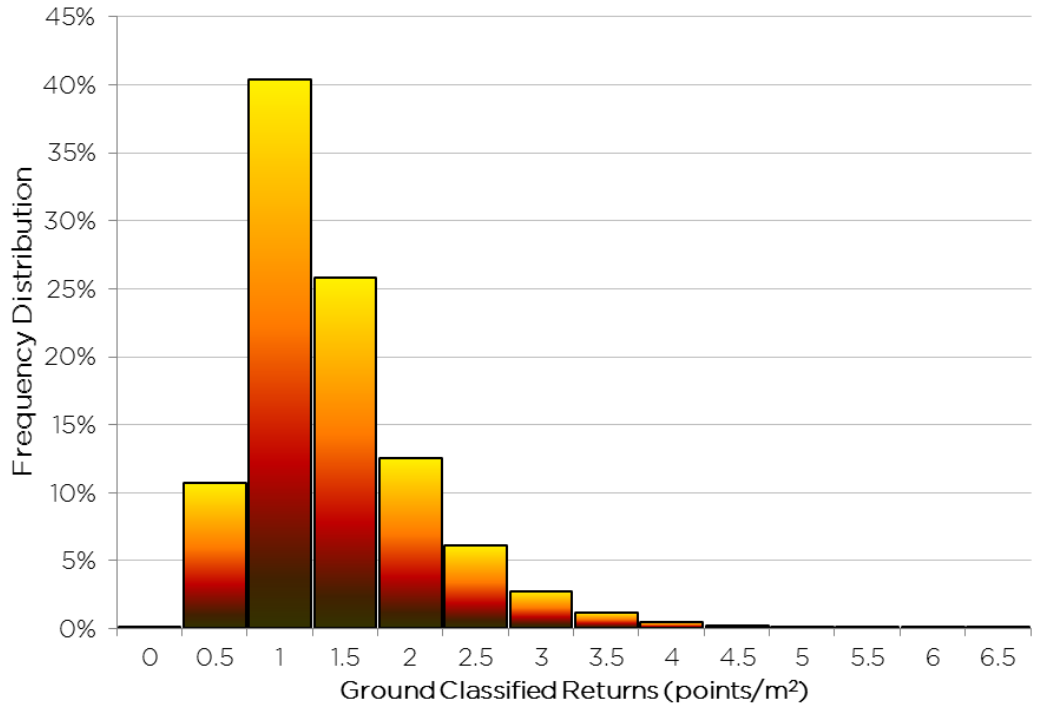

**Figure 11.** First return density distribution map for the Powell AOI

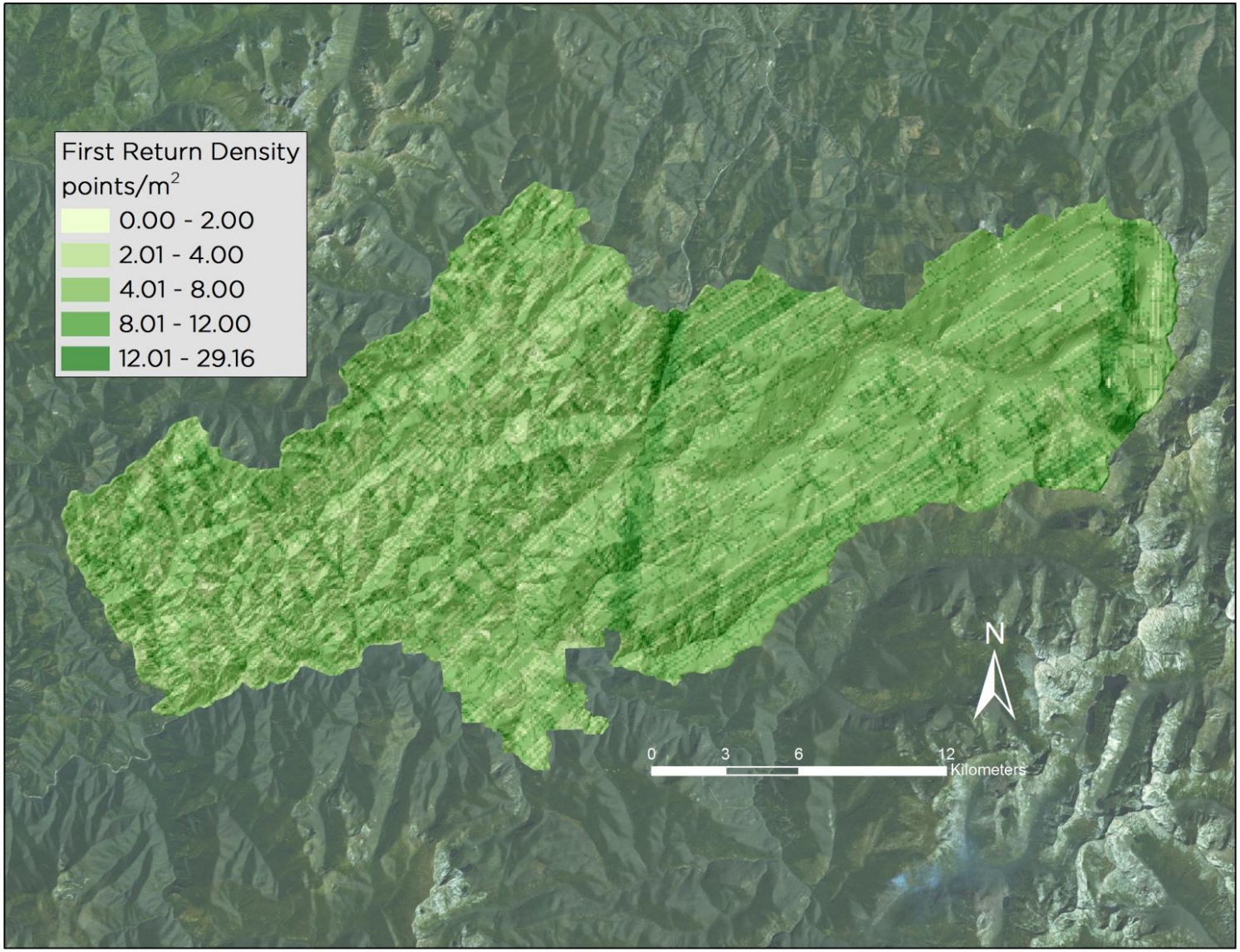

Figure 12. Ground density distribution map for the Powell AOI

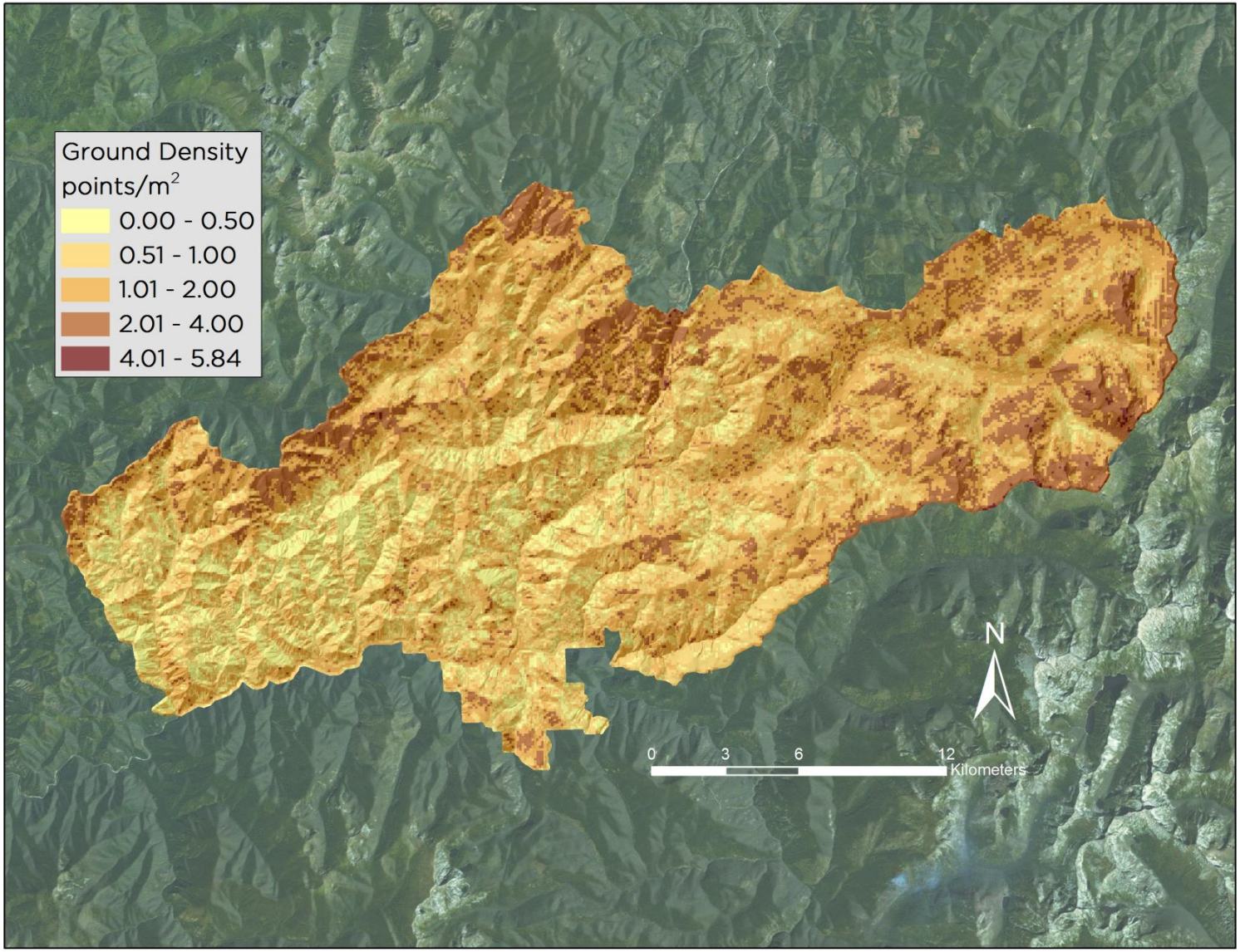

Figure 13. First return density distribution map for the Corral Creek, Hog Meadow, and Potlatch River AOI

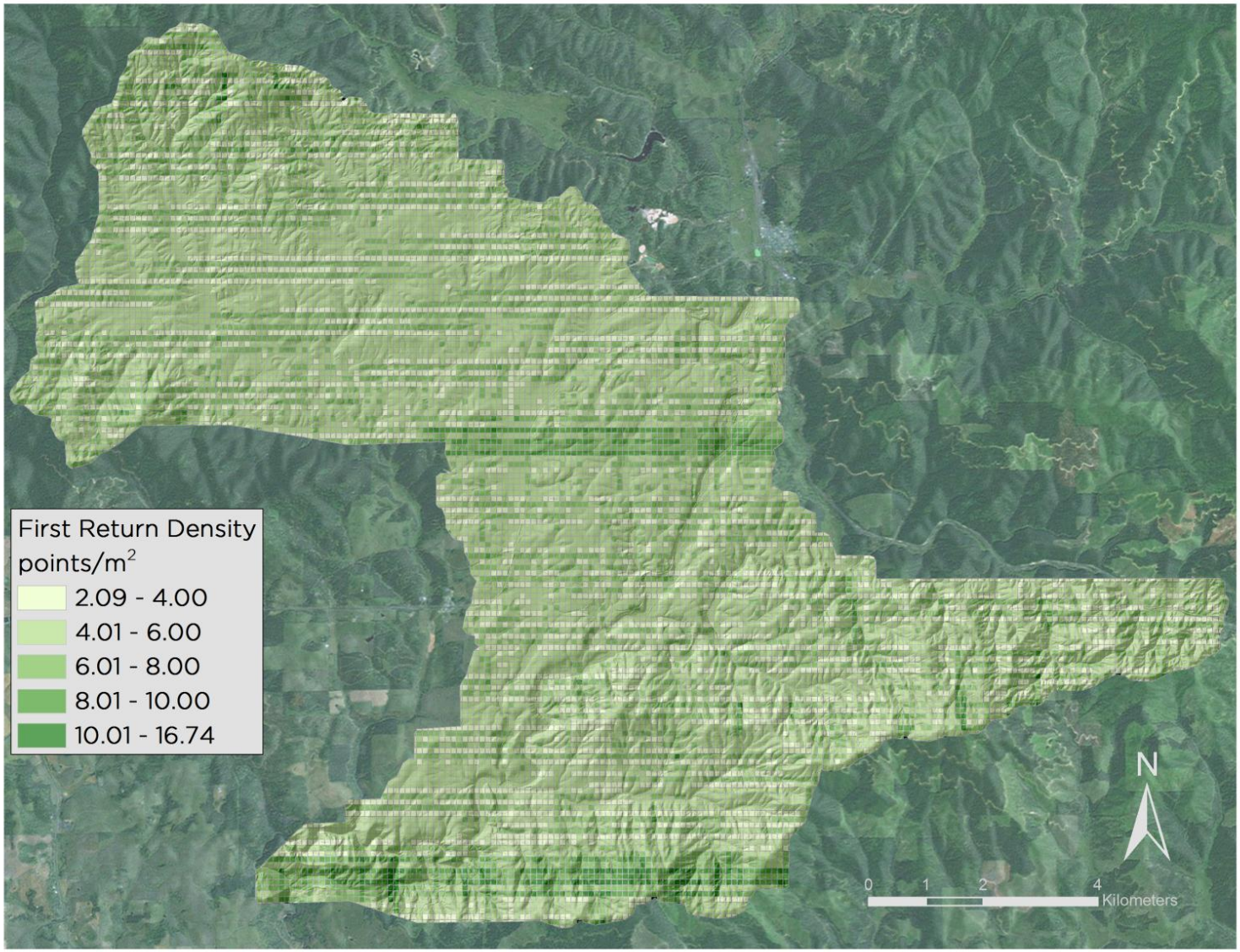

Figure 14. Ground density distribution map for the Corral Creek, Hog Meadow, and Potlatch River AOI

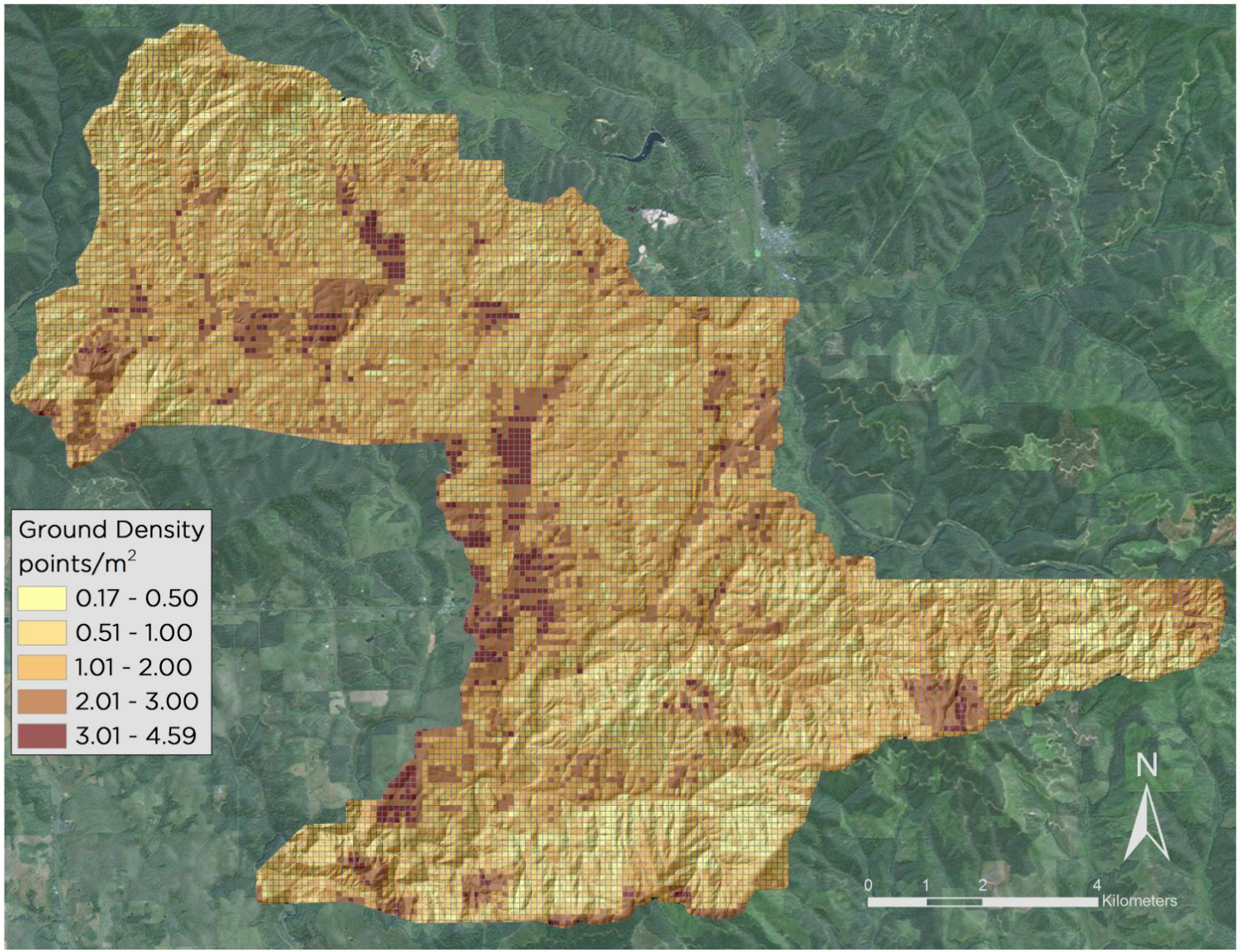

Figure 15. First return density distribution map for the Crooked River AOI

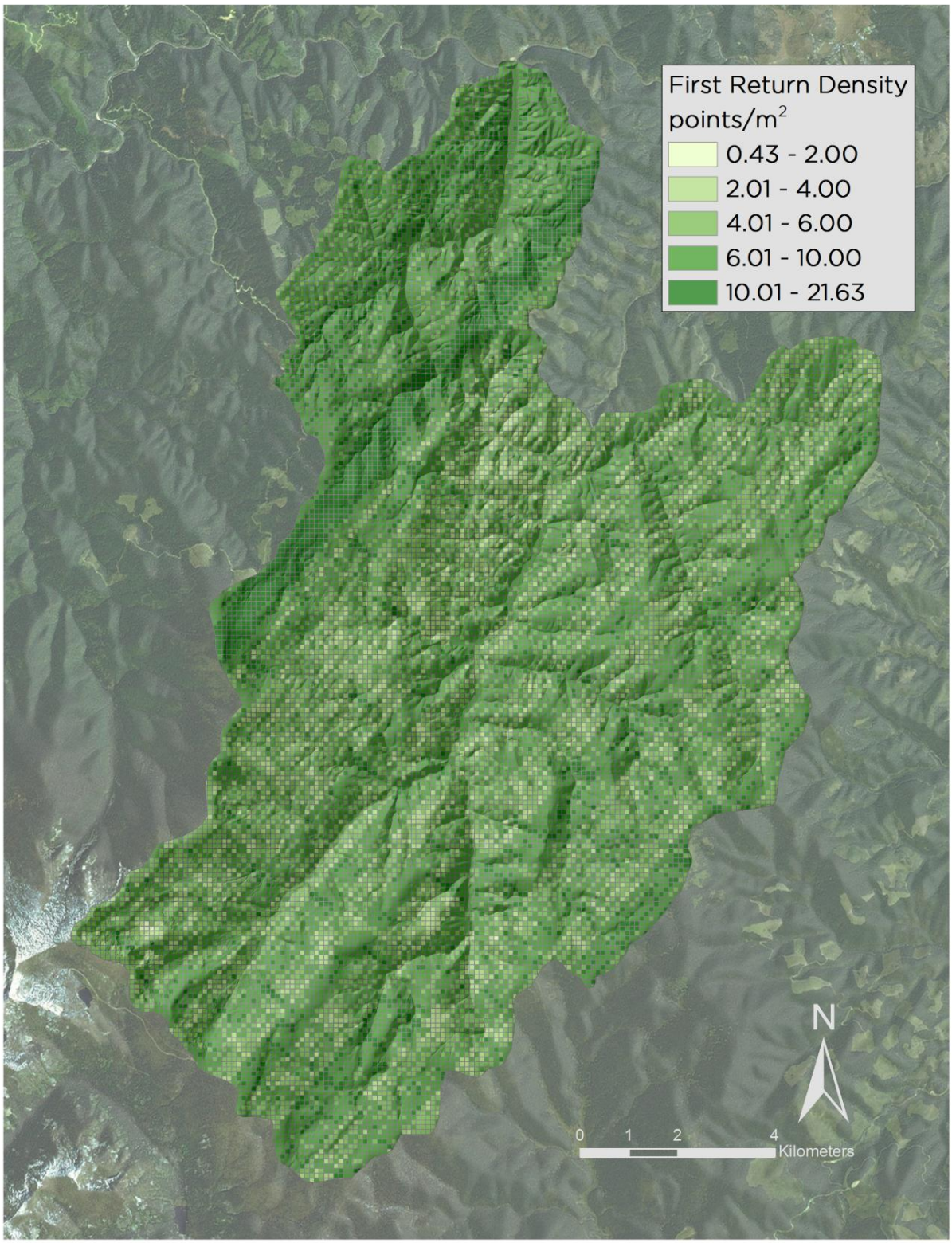

Figure 16. Ground density distribution map for the Crooked River AOI

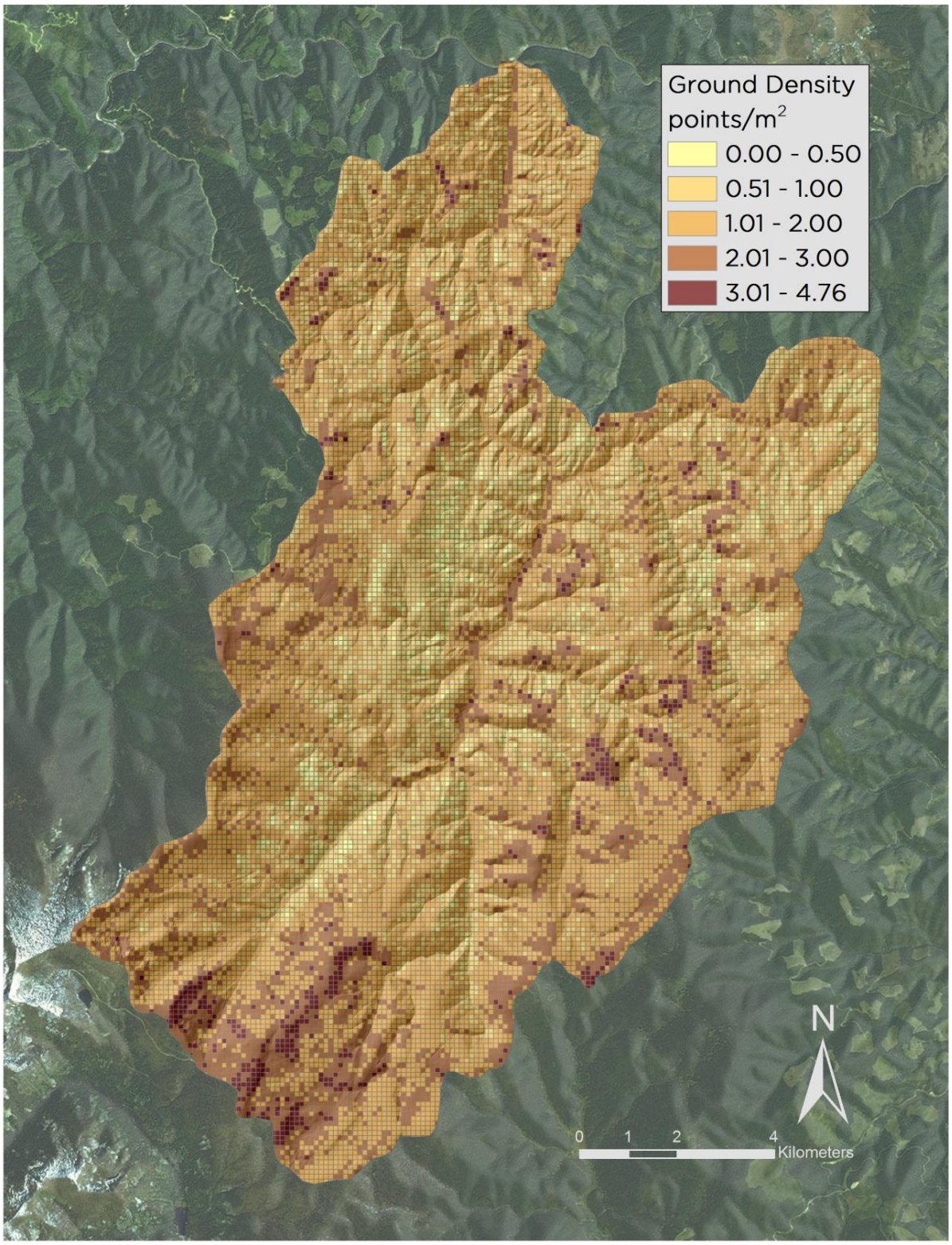

Figure 17. First return density distribution map for the Hungry Ridge and Mill Creek AOI

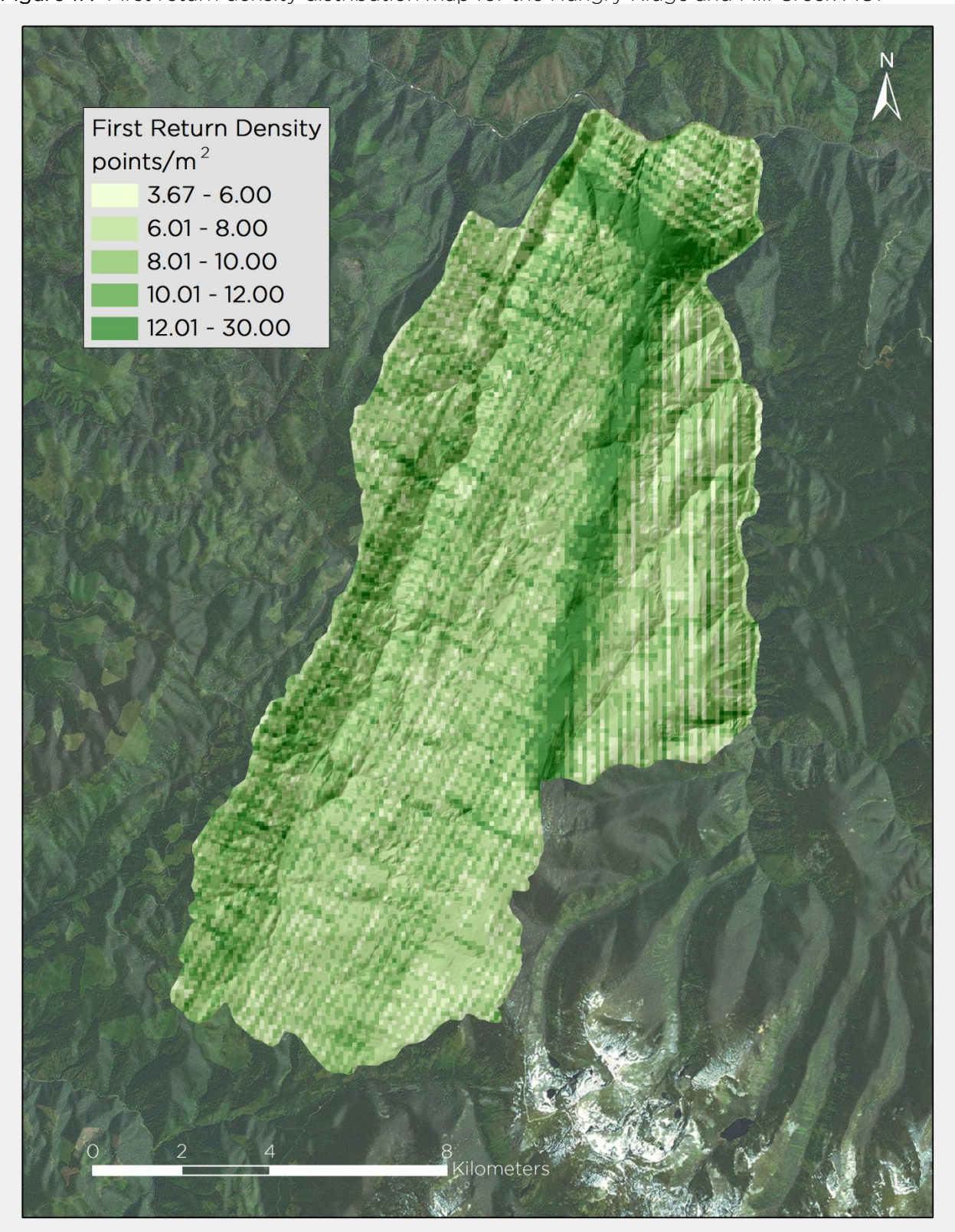

Figure 18. Ground density distribution map for the Hungry Ridge and Mill Creek AOI

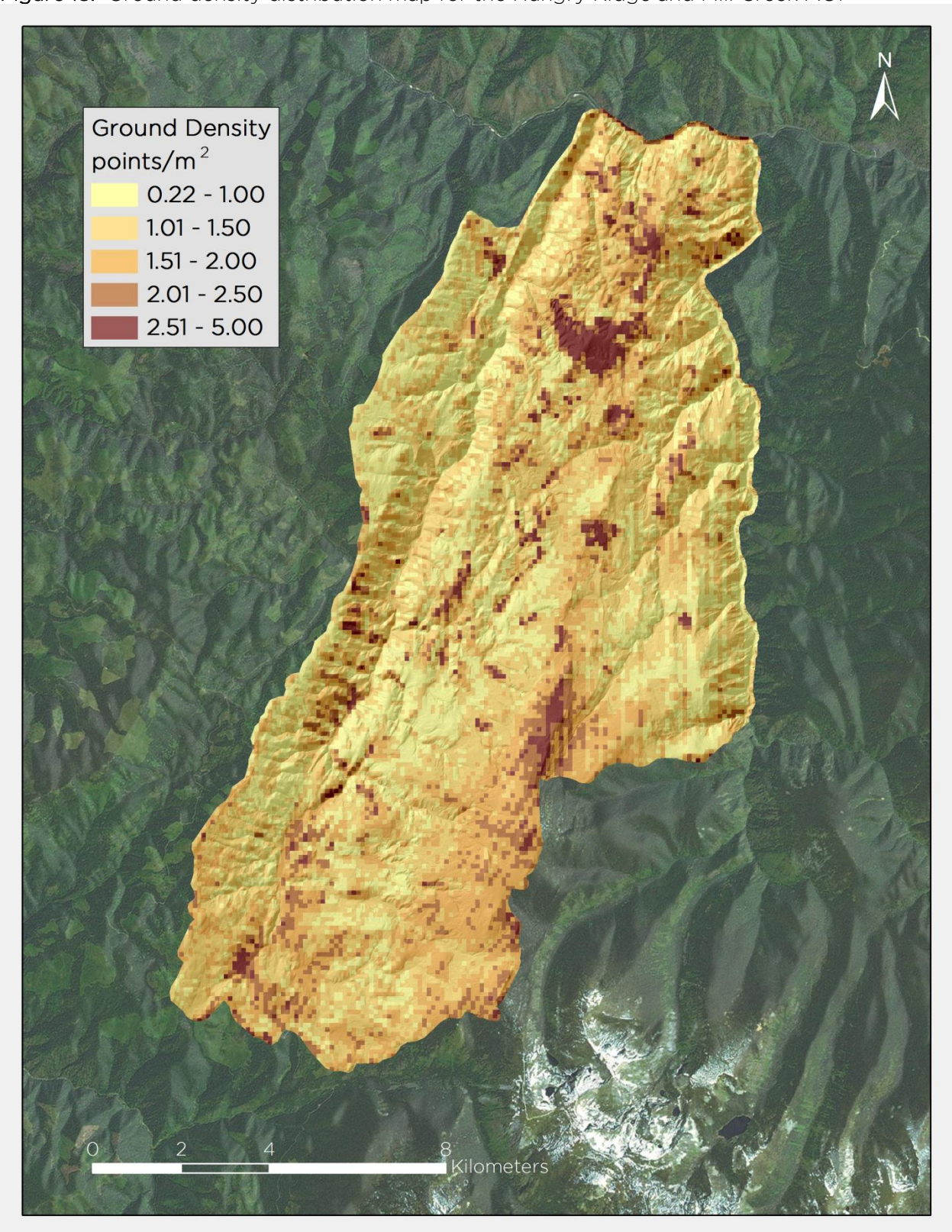

Figure 19. First return density distribution map for the Selway and Elk Creek AOI

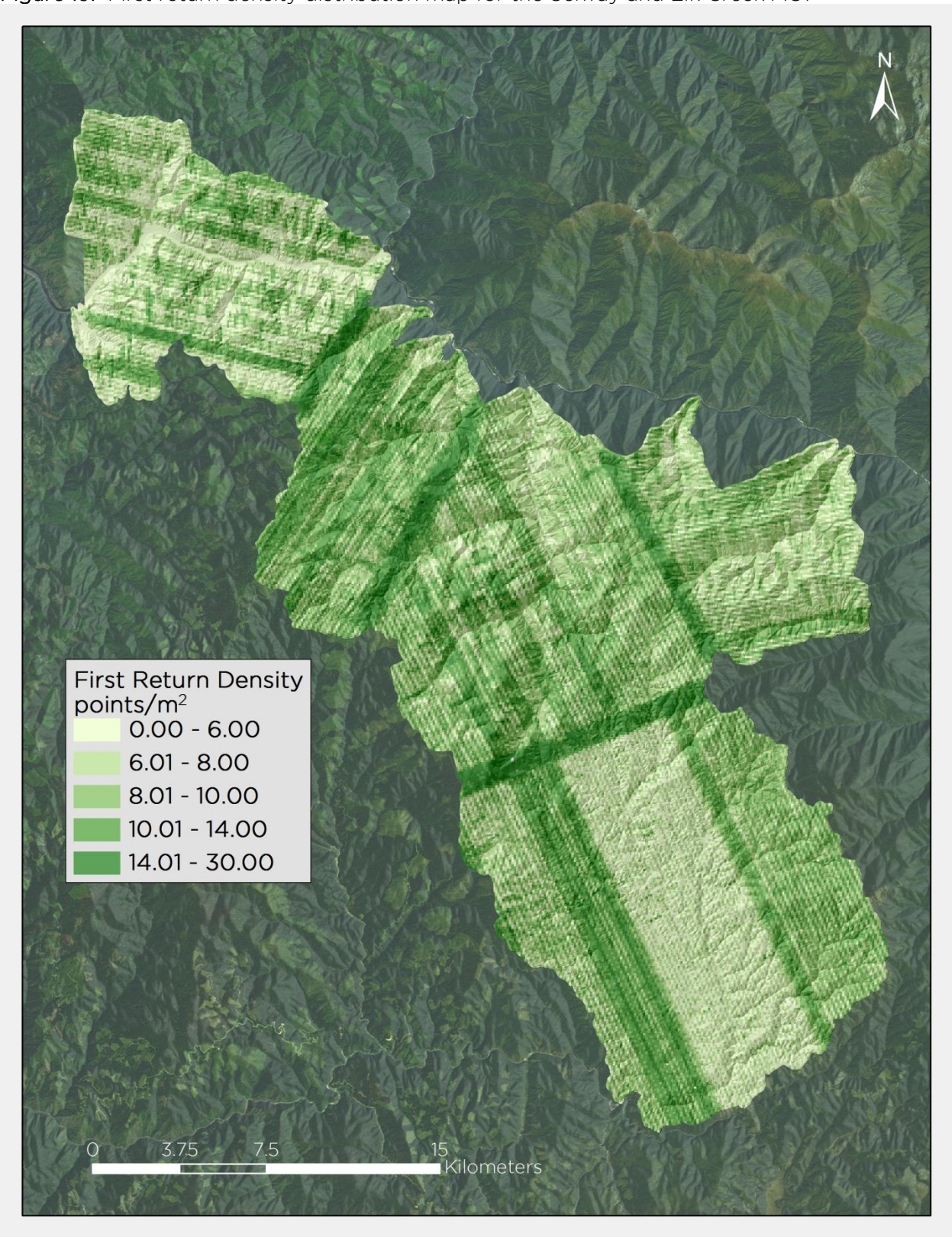

Figure 20. Ground density distribution map for the Selway and Elk Creek AOI

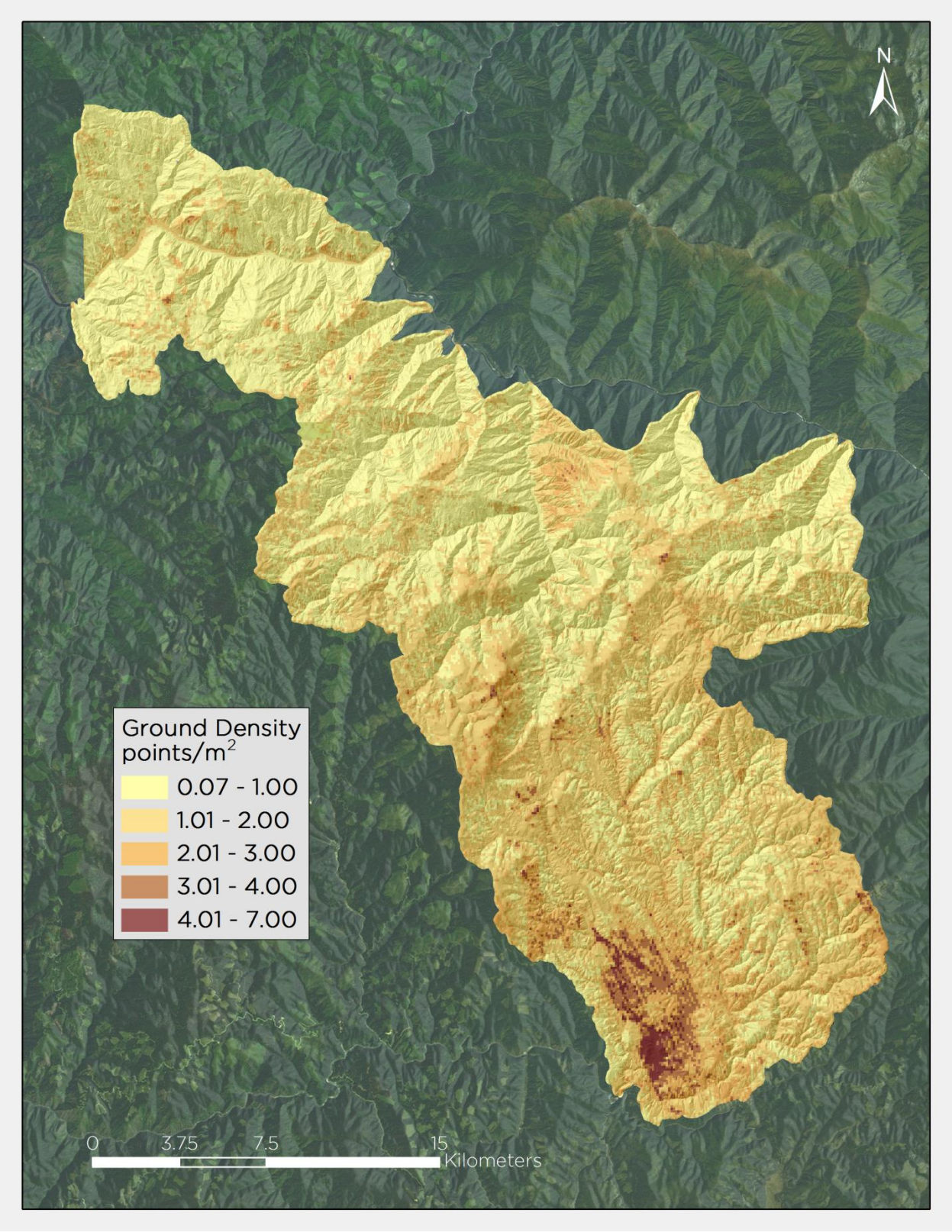

Figure 21. First return density distribution map for the French Preacher and North Fork AOI

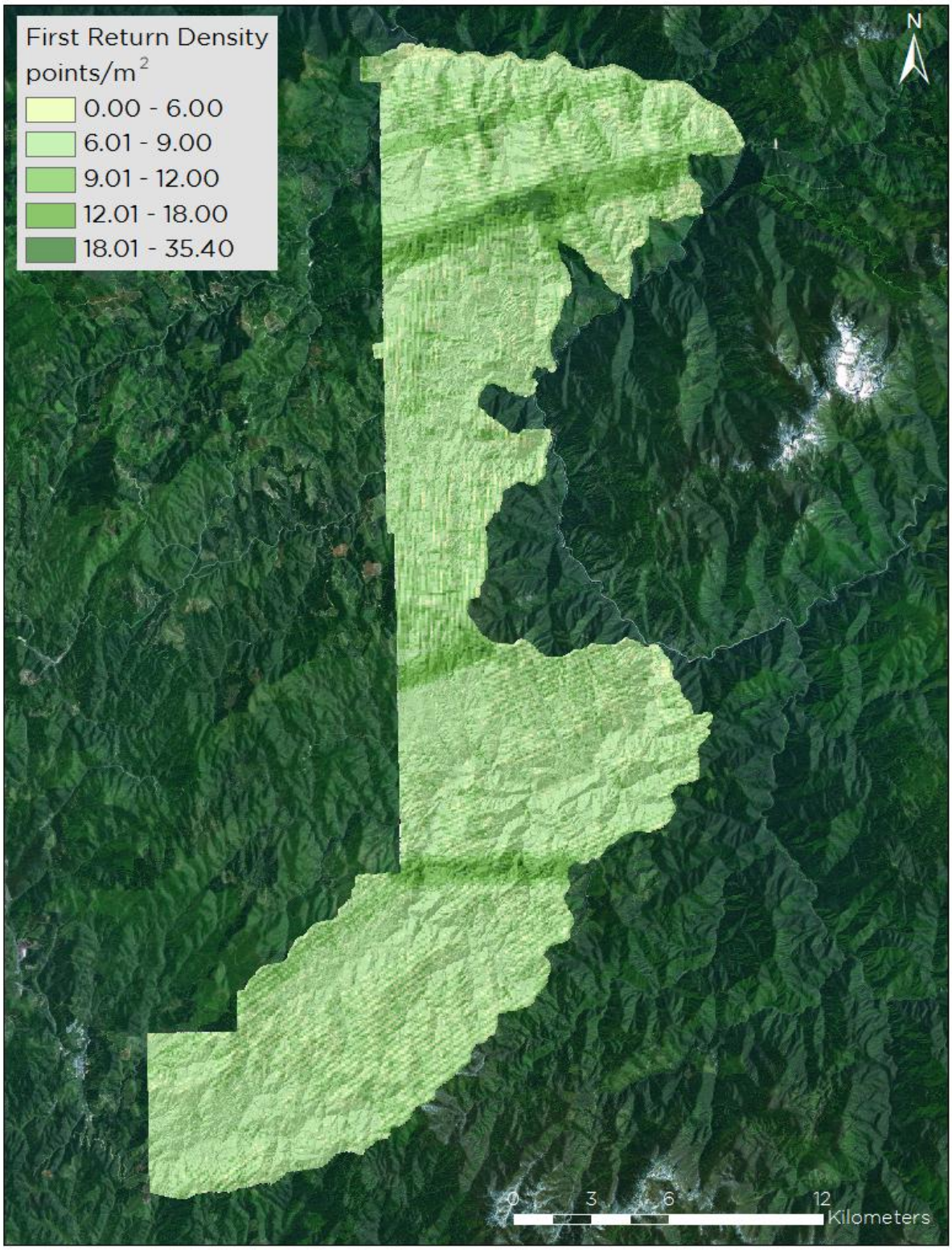

Figure 22. Ground density distribution map for the French Preacher and North Fork AOI

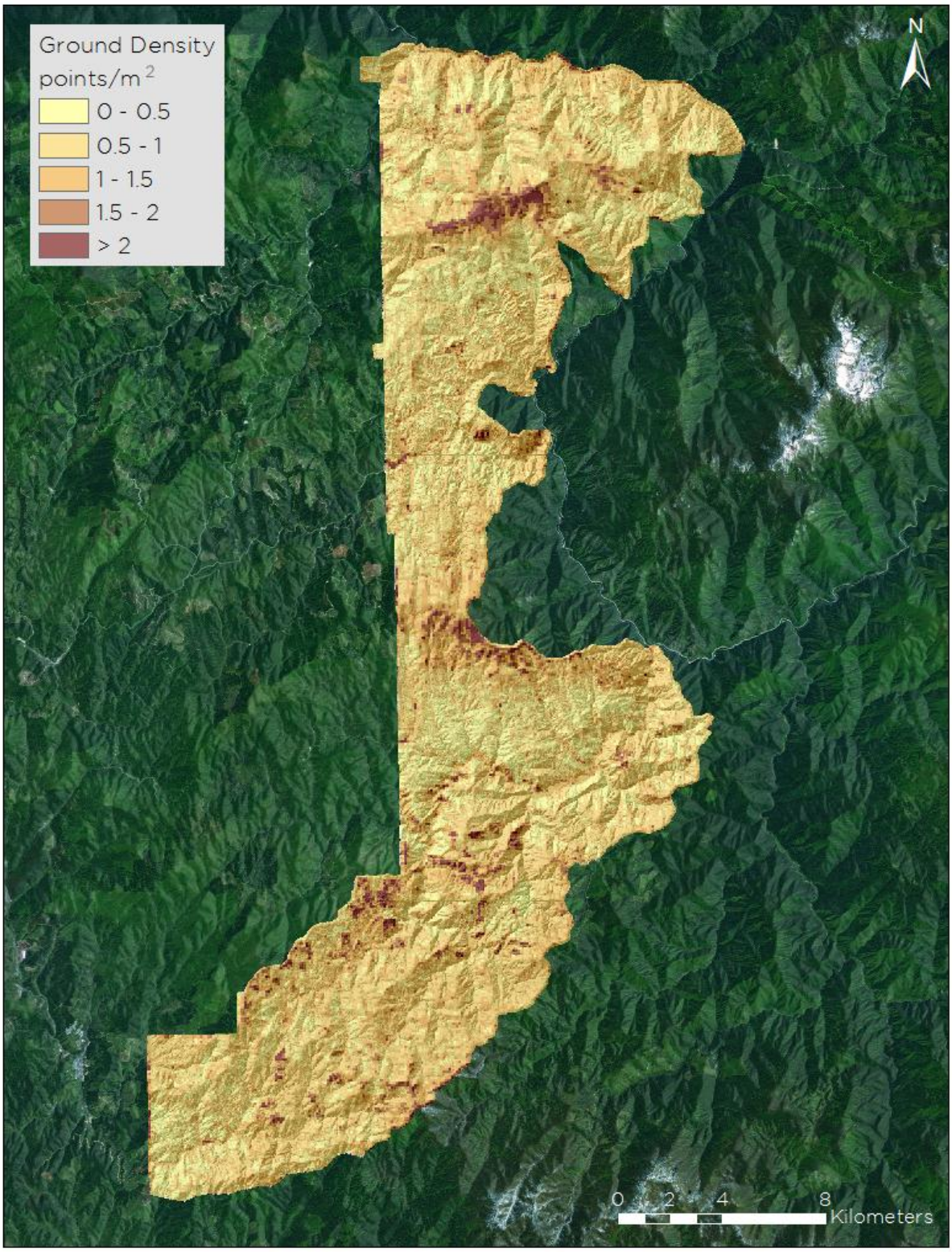

Figure 23. First return density distribution map for the Eldorado/Lolo AOI

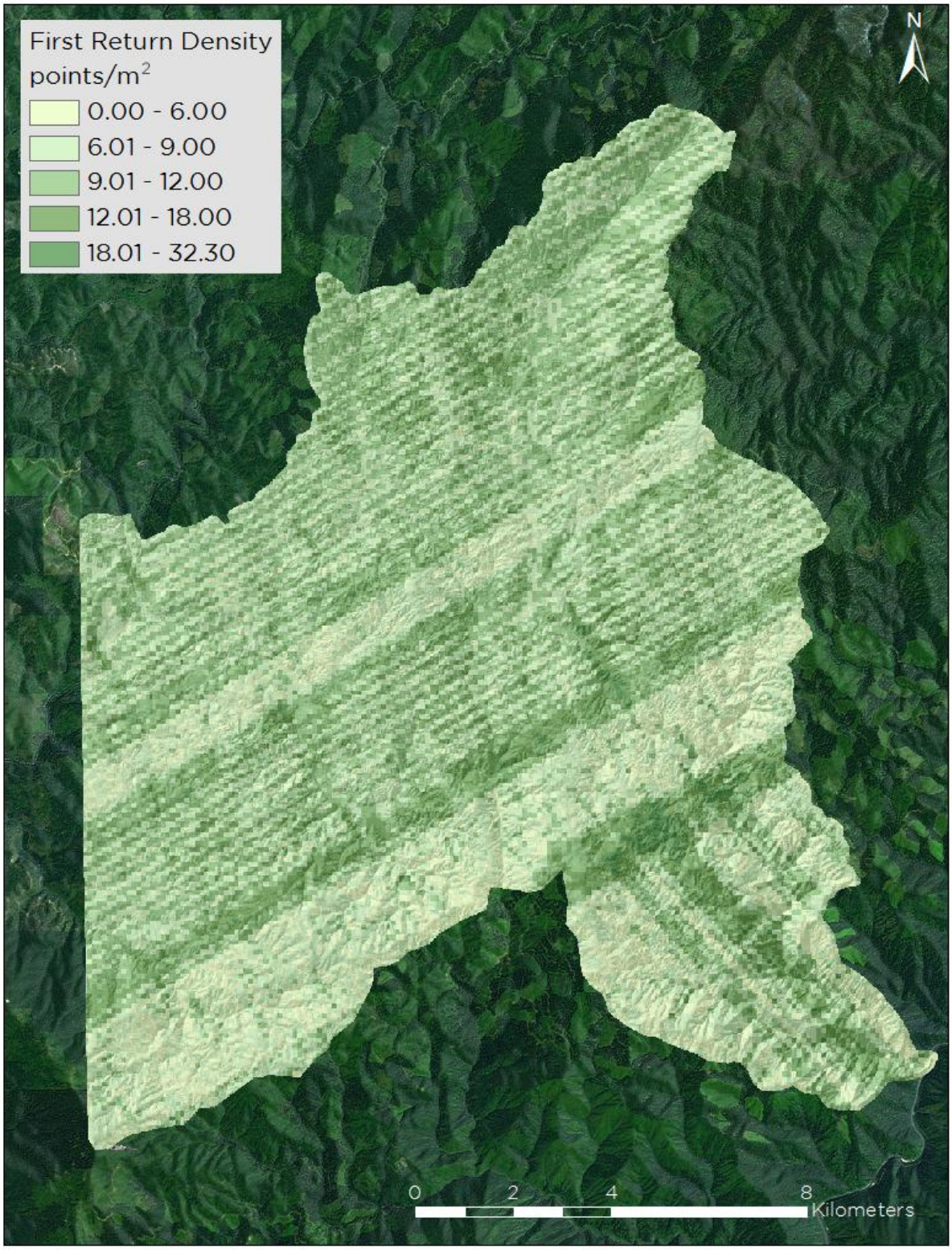

Figure 24. Ground density distribution map for the Eldorado/Lolo AOI

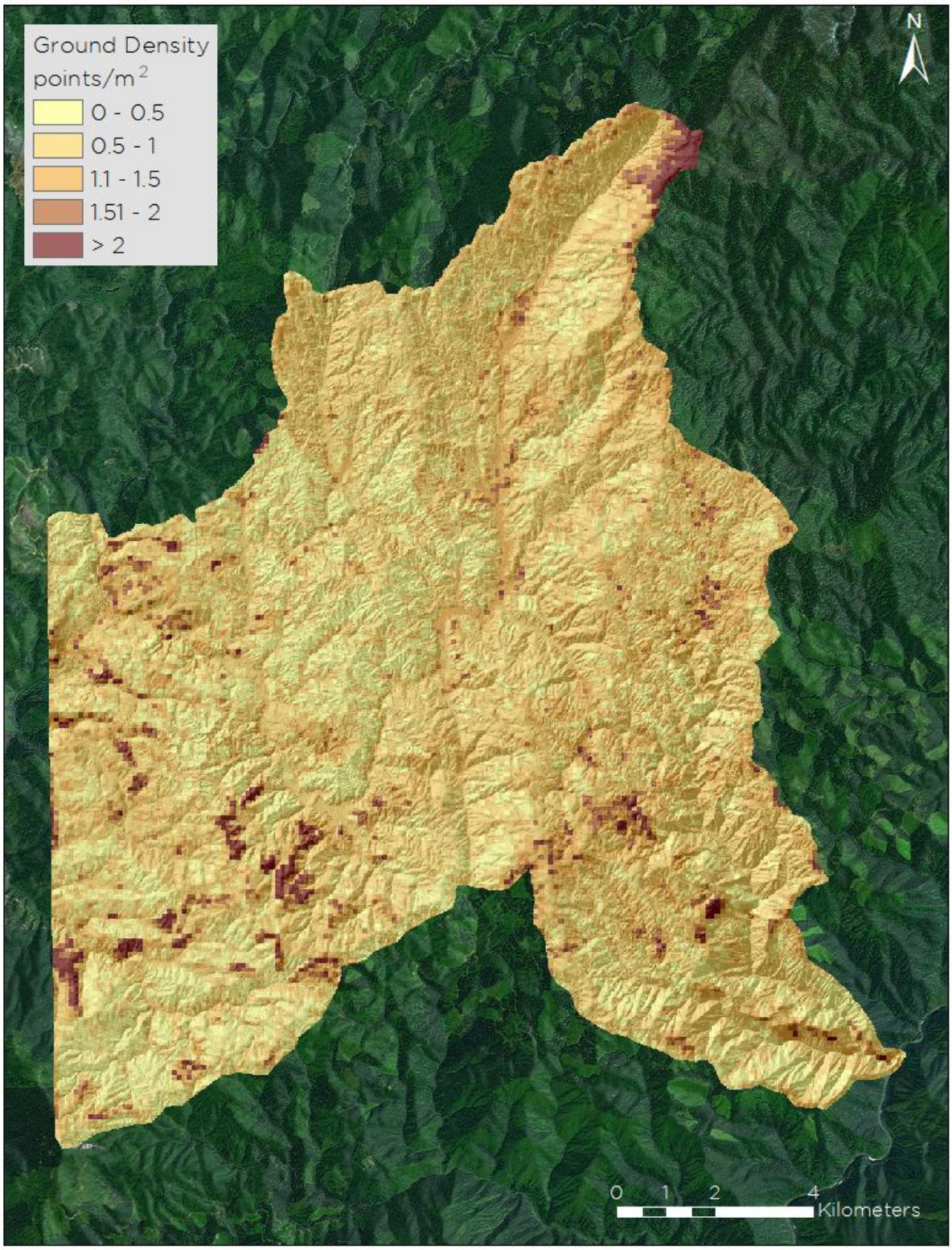

## 5.3 Relative Accuracy Calibration Results

Relative accuracy statistics for the Nez Perce and Clearwater National Forests' datasets measure the full survey calibration including areas outside the delivered boundary (Table 4, Figure 25).

**Table 4.** Relative Accuracy – Deviation between laser points and RTK hard surface survey points (all statistics in meters).

| | Average | RMSE | Median | 1 sigma (σ) | 1.96 sigma (σ) |
|---|---|---|---|---|---|
| Powell | 0.072 | 0.074 | 0.073 | 0.009 | 0.017 |
| Crooked River | 0.054 | 0.055 | 0.054 | 0.006 | 0.013 |
| Corral Creek<br>Hog Meadow<br>Potlatch River | 0.055 | 0.060 | 0.051 | 0.017 | 0.034 |
| Hungry Ridge<br>Mill Creek | 0.063 | 0.067 | 0.062 | 0.012 | 0.024 |
| Selway<br>Elk | 0.056 | 0.067 | 0.064 | 0.013 | 0.026 |
| French Preacher<br>North Fork | 0.033 | 0.033 | 0.033 | 0.006 | 0.011 |
| Eldorado<br>Lolo | 0.064 | 0.072 | 0.061 | 0.019 | 0.036 |

**Figure 25.** Distribution of relative accuracies per flight line all AOIs within the Nez Perce and Clearwater National Forests, non-slope adjusted

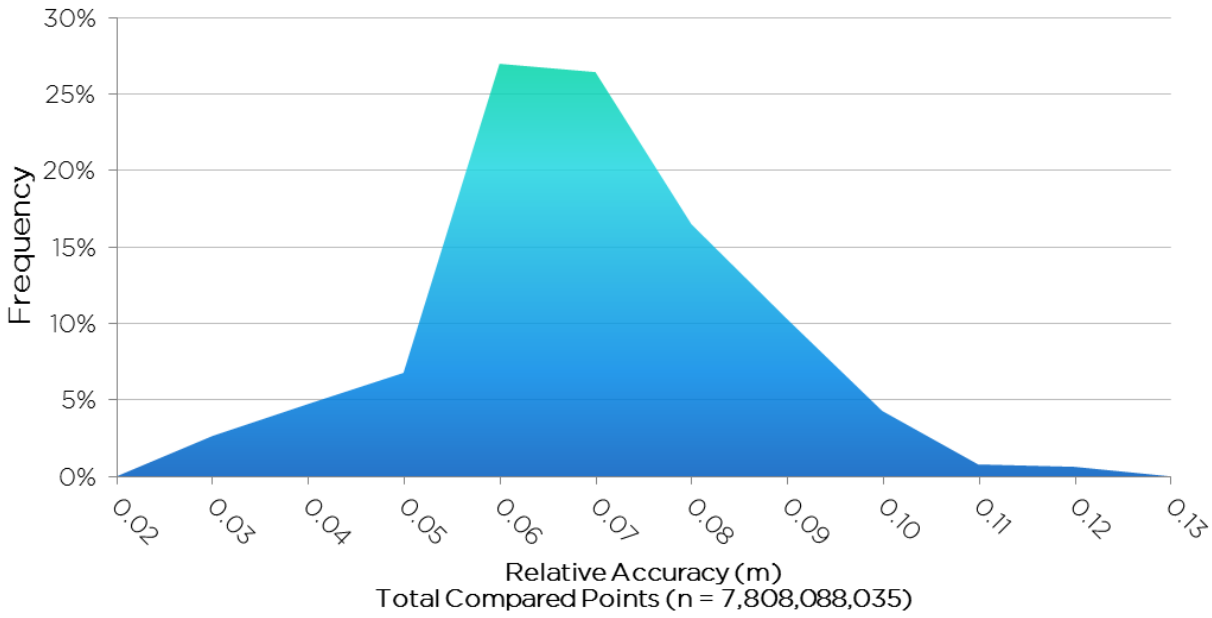

## 5.4 Absolute Accuracy Results

Table 5 shows absolute accuracies for the Nez Perce and Clearwater National Forest by AOI. Figure 26 shows the cumulative absolute accuracy for all AOIs in the study area.

**Table 5.** Absolute Accuracy – Deviation between laser points and RTK hard surface survey points (all statistics in meters).

| | RTK (n) | Average | RMSE | Minimum | Maximum | 1 sigma (σ) | 1.96 sigma (σ) |
|---|---|---|---|---|---|---|---|
| Powell | 1,460 | -0.009 | 0.038 | -0.119 | 0.090 | 0.037 | 0.072 |
| Crooked River | 583 | 0.020 | 0.025 | -0.088 | 0.081 | 0..025 | 0.050 |
| Corral Creek<br>Hog Meadow<br>Potlatch River | 334 | 0.000 | 0.042 | -0.095 | 0.122 | 0.042 | 0.082 |
| Hungry Ridge<br>Mill Creek | 188 | 0.001 | 0.036 | -0.127 | 0.075 | 0.036 | 0.070 |
| Selway<br>Elk | 1,428 | -0.009 | 0.034 | -0.137 | 0.105 | 0.033 | 0.065 |
| French Preacher<br>North Fork | 1034 | 0.019 | 0.024 | -0.113 | 0.063 | 0.024 | 0.046 |
| Eldorado<br>Lolo | 363 | 0.000 | 0.036 | -0.108 | 0.150 | 0.036 | 0.070 |

**Figure 26.** Cumulative Absolute Accuracy Histogram for all AOIs in the Nez Perce and Clearwater National Forests

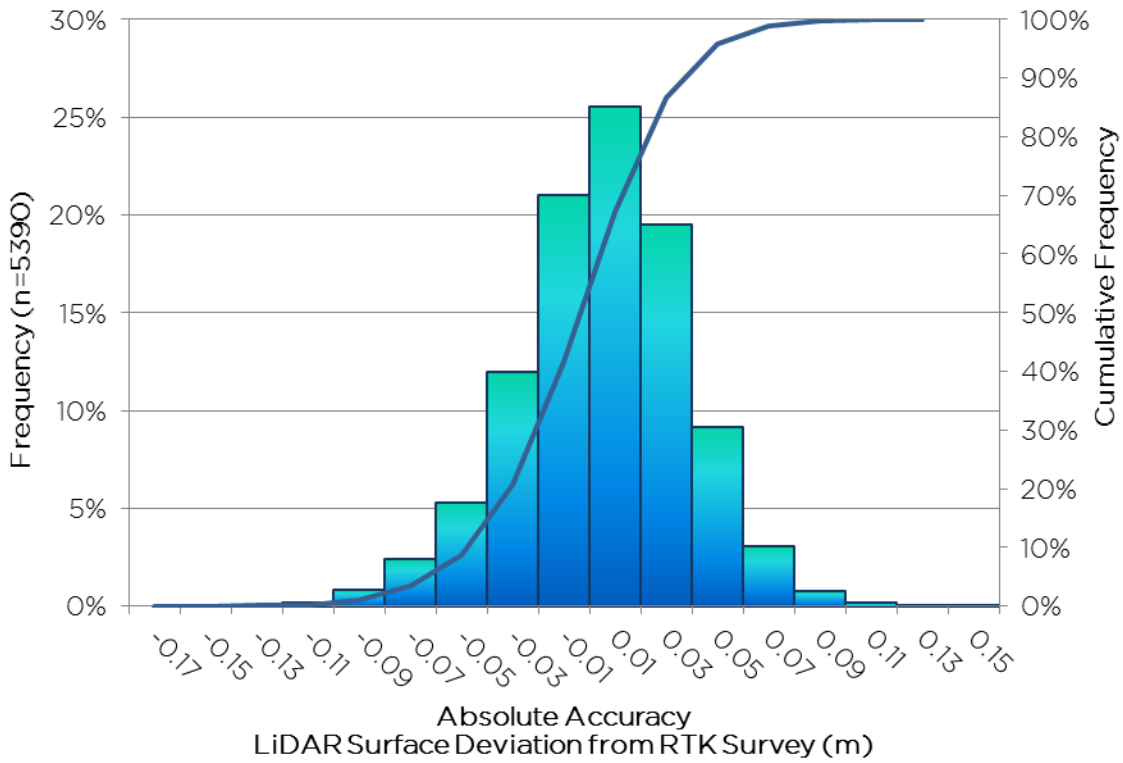

In addition to RTK, land cover check points were taken throughout the entire study area. Land cover types and descriptions can be referenced in Table 6. Tables 7-13 show the land cover statistics by AOI.

Table 6. Landcover descriptions of check points taken within the Nez Perce and Clearwater National Forests

| Land Cover | Description |
|---|---|
| Evergreen/ Sparse Forest/ Trees | Areas with sparse coniferous and or deciduous tree coverage characterized by an open canopy. RTK points were acquired as close to the tree base as possible with PDOP less than 3.0 and RMS less than 0.2 meters. |
| Hard Surface | Surfaces that include dirt, gravel, and paved roadways. |
| Short Grass | Grass heights that are below the knee. Points were taken with RTK pole in the center of the grass patch. |
| Shrub | Areas characterized by natural or semi-natural woody vegetation with aerial stems that are generally less than 6 meters tall, with individuals or clumps not touching or interlocking. Both evergreen and deciduous species of true shrubs, young trees, and trees or shrubs that are small or stunted because of environmental conditions are included. |
| Tall Grass | Grass heights that are above the knee. Points were taken with the RTK pole in the center of the grass patch. |

Table 7. Land Cover statistics for the Powell AOI

| Land Cover | Sample Size (n) | Mean Dz | 1 sigma (σ) | 1.96 sigma (σ) | RMSE |
|---|---|---|---|---|---|
| Hard Surface | 1,460 | -0.009m | 0.037m | 0.072m | 0.038m |
| Short Grass | 9 | 0.032m | 0.031m | 0.061m | 0.044m |
| Tall Grass | 20 | 0.065m | 0.093m | 0.181m | 0.111m |
| Shrubs | 19 | 0.089m | 0.150m | 0.294m | 0.171m |
| Trees | 20 | 0.075m | 0.119m | 0.234m | 0.139m |

Table 8. Land Cover statistics for the Crooked River AOI

| Land Cover | Sample Size (n) | Mean Dz | 1 sigma (σ) | 1.96 sigma (σ) | RMSE |
|---|---|---|---|---|---|
| Hard Surface | 584 | 0.002m | 0.027m | 0.053m | 0.027m |
| Evergreen/ Sparse Forest/ Trees | 26 | -0.003m | 0.051m | 0.102m | 0.051m |
| Tall Grass | 25 | 0.037m | 0.087m | 0.171m | 0.093m |

Table 9. Land Cover statistics for the Corral Creek, Hog Meadow, and Potlatch River AOI

| Land Cover | Sample Size (n) | Mean Dz | 1 sigma (σ) | 1.96 sigma (σ) | RMSE |
|---|---|---|---|---|---|
| Hard Surface | 334 | -0.003m | 0.042m | 0.082m | 0.042m |
| Short Grass | 31 | 0.021m | 0.037m | 0.072m | 0.042m |
| Tall Grass | 8 | 0.046m | 0.027m | 0.053m | 0.052m |
| Evergreen/ Sparse Forest/ Trees | 25 | -0.211m | 0.111m | 0.217m | 0.110m |

Table 10. Land Cover statistics for the Hungry Ridge and Mill Creek River AOI

| Land Cover | Sample Size (n) | Mean Dz | 1 sigma (σ) | 1.96 sigma (σ) | RMSE |
|---|---|---|---|---|---|
| Evergreen/ Sparse Forest/ Trees | 23 | -0.006m | 0.039m | 0.076m | 0.038m |
| Short Grass | 23 | -0.002m | 0.033m | 0.064m | 0.032m |
| Tall Grass | 21 | 0.048m | 0.037m | 0.072m | 0.060m |

Table 11. Land Cover statistics for the Selway and Elk AOI

| Land Cover | Sample Size (n) | Mean Dz | 1 sigma (σ) | 1.96 sigma (σ) | RMSE |
|---|---|---|---|---|---|
| Evergreen/ Sparse Forest/ Trees | 56 | 0.043m | 0.040m | 0.078m | 0.059m |
| Short Grass | 34 | 0.028m | 0.024m | 0.048m | 0.037m |
| Tall Grass | 27 | 0.070m | 0.057m | 0.110m | 0.090m |
| Shrubs | 36 | 0.071m | 0.060m | 0.118m | 0.121m |

Table 12. Land Cover statistics for the French Preacher and North Fork AOI

| Land Cover | Sample Size (n) | Mean Dz | 1 sigma (σ) | 1.96 sigma (σ) | RMSE |
|---|---|---|---|---|---|
| Trees | 50 | 0.000m | 0.041m | 0.081m | 0.058m |
| Short Grass | 38 | -0.006m | 0.020m | 0.039m | 0.029m |
| Tall Grass | 26 | 0.071m | 0.066m | 0.130m | 0.104m |
| Shrub | 24 | 0.058m | 0.085m | 0.166m | 0.110m |

Table 13. Land Cover statistics for the Eldorado and Lolo AOI

| Land Cover | Sample Size (n) | Mean Dz | 1 sigma (σ) | 1.96 sigma (σ) | RMSE |
|---|---|---|---|---|---|
| Trees | 30 | 0.042m | 0.032m | 0.063m | 0.057m |
| Short Grass | 27 | 0.028m | 0.029m | 0.056m | 0.052m |
| Shrubs | 20 | 0.039m | 0.028m | 0.056m | 0.057m |

## 6. Projection/Datum and Units

| | | |
|---|---|---|
| Projection | | UTM Zone 11, Meters |
| Datum | Vertical: | NAVD88 Geoid03 |
| | Horizontal: | NAD83 (CORS96) |
| Units | | Meters |

## 7. Deliverables

| | |
|---|---|
| Point Data | •All laser returns classified to ground (LAS v. 1.2 format; 750m$^2$ tile delineation) |
| Vector Data | •Total area flown (ESRI shapefile format)<br>•LiDAR Index (ESRI shapefile format)<br>•Total area flown (ESRI shapefile format) |
| Raster Data | •Bare Earth Model (1m ESRI GRID and ERDAS Image format)<br>•Vegetation Canopy Model (1m ESRI GRID and ERDAS Image format)<br>•Intensity Image (GeoTIFF format, 0.5m resolution) |
| Data Report | •Full report containing introduction, methodology, and accuracy |

## 8. Selected Images

Figure 27. View looking South at the hills above Sneak Creek. The top image is the 3D LiDAR point cloud colored by NAIP imagery, the bottom image is the bare-earth model colored by elevation.

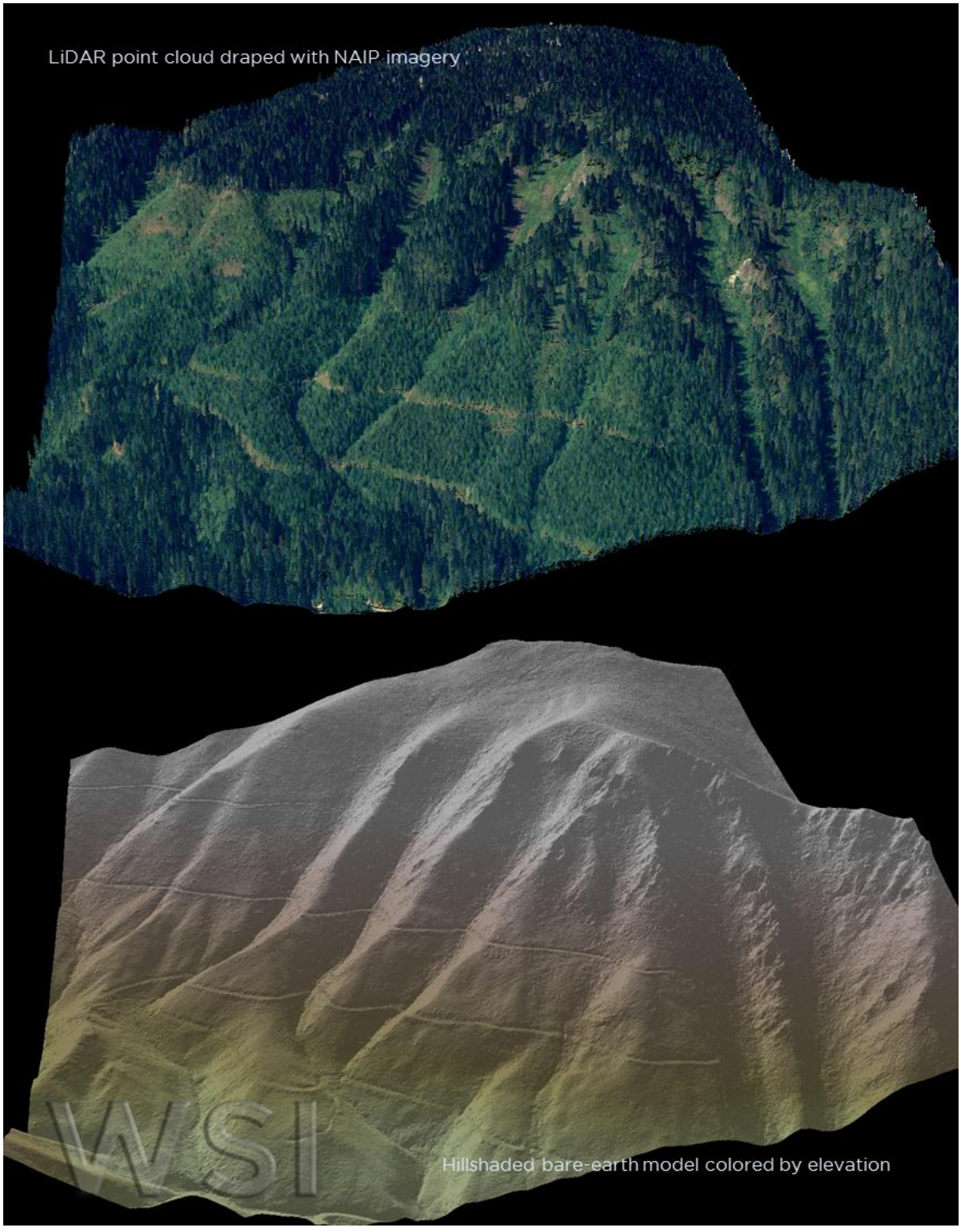

Figure 28. Bare-earth hillshaded model of Orogrande Creek colored by elevation.

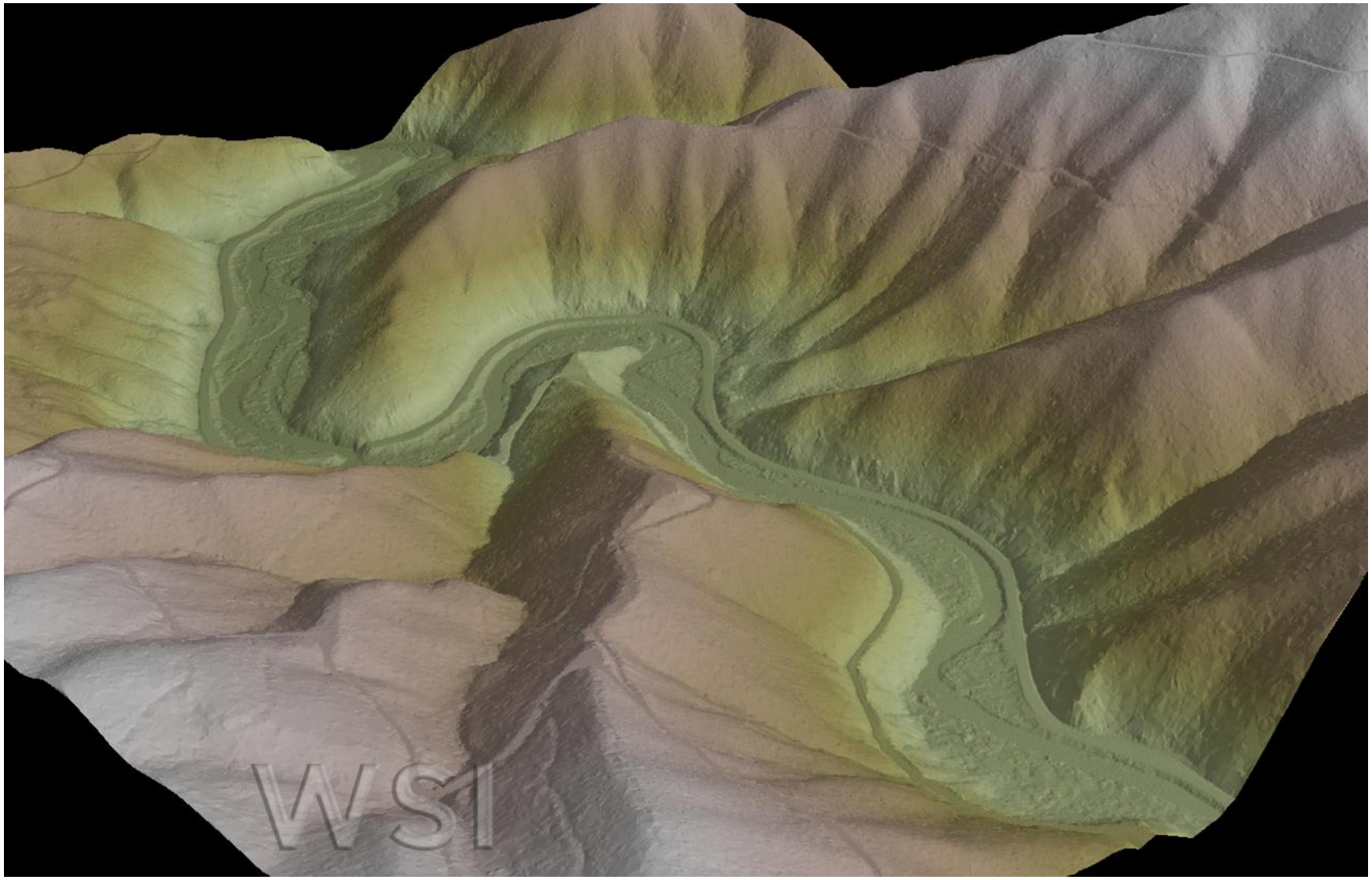

Figure 29. 3D LiDAR point cloud of a cross section of Orogrande Creek. The points are draped with 2011 NAIP imagery.

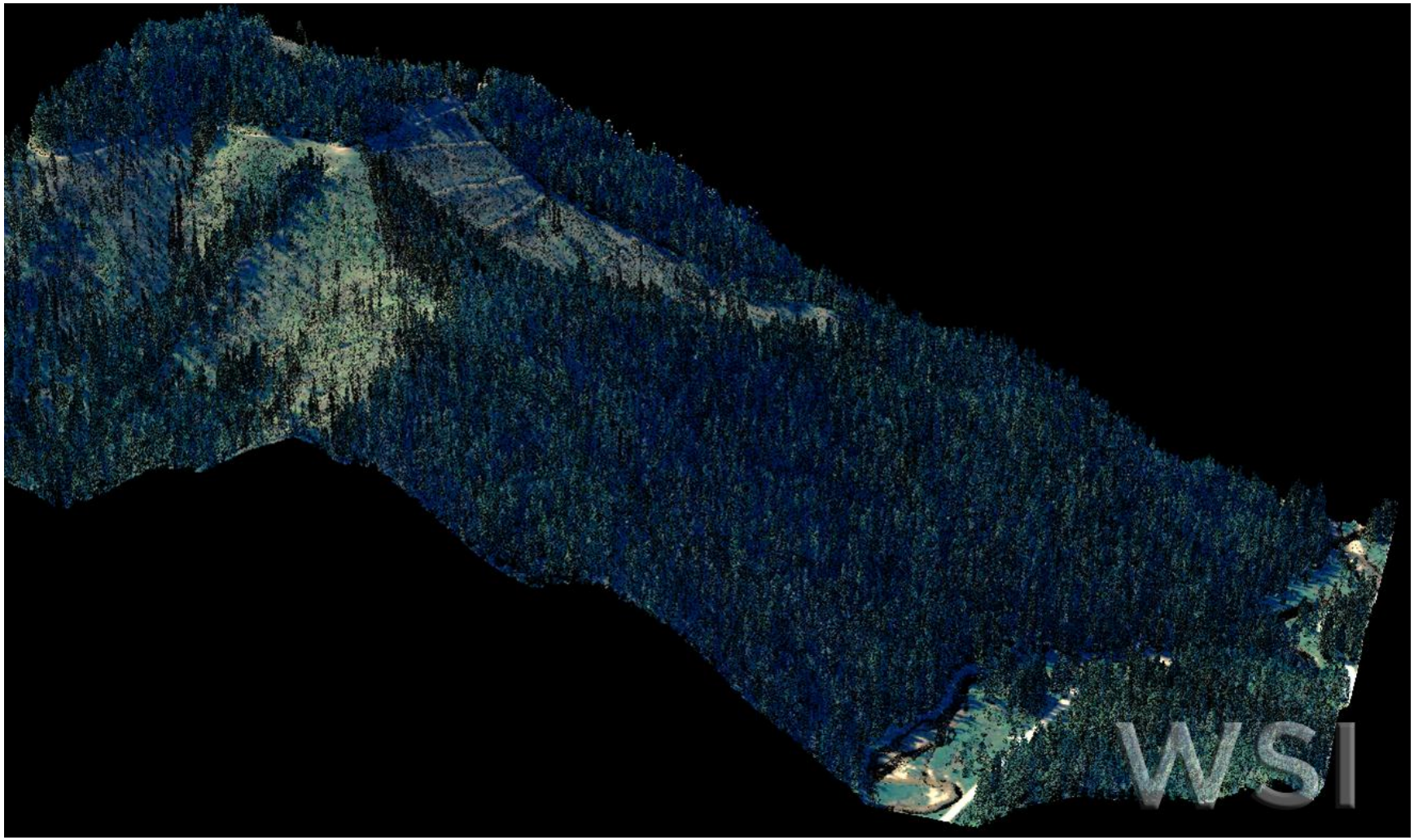

# 9. Glossary

1-sigma (σ) Absolute Deviation: Value for which the data are within one standard deviation (approximately 68$^{th}$ percentile) of a normally distributed data set.
1.96-sigma (σ) Absolute Deviation: Value for which the data are within two standard deviations (approximately 95$^{th}$ percentile) of a normally distributed data set.
Root Mean Square Error (RMSE): A statistic used to approximate the difference between real-world points and the LiDAR points. It is calculated by squaring all the values, then taking the average of the squares and taking the square root of the average.
Pulse Rate (PR): The rate at which laser pulses are emitted from the sensor; typically measured as thousands of pulses per second (kHz).
Pulse Returns: For every laser pulse emitted, the Leica ALS 60 system can record *up to four* wave forms reflected back to the sensor. Portions of the wave form that return earliest are the highest element in multi-tiered surfaces such as vegetation. Portions of the wave form that return last are the lowest element in multi-tiered surfaces.
Accuracy: The statistical comparison between known (surveyed) points and laser points. Typically measured as the standard deviation (sigma, σ) and root mean square error (RMSE).
Intensity Values: The peak power ratio of the laser return to the emitted laser. It is a function of surface reflectivity.
Data Density: A common measure of LiDAR resolution, measured as points per square meter.
Spot Spacing: Also a measure of LiDAR resolution, measured as the average distance between laser points.
Nadir: A single point or locus of points on the surface of the earth directly below a sensor as it progresses along its flight line.
Scan Angle: The angle from nadir to the edge of the scan, measured in degrees. Laser point accuracy typically decreases as scan angles increase.
Overlap: The area shared between flight lines, typically measured in percents; 100% overlap is essential to ensure complete coverage and reduce laser shadows.
DTM / DEM: These often-interchanged terms refer to models made from laser points. The digital elevation model (DEM) refers to all surfaces, including bare ground and vegetation, while the digital terrain model (DTM) refers only to those points classified as ground.
Real-Time Kinematic (RTK) Survey: GPS surveying is conducted with a GPS base station deployed over a known monument with a radio connection to a GPS rover. Both the base station and rover receive differential GPS data and the baseline correction is solved between the two. This type of ground survey is accurate to 1.5 cm or less.

# 10. Citations

Soininen, A. 2004. TerraScan User's Guide. TerraSolid.

# Appendix A

Laser Noise
For any given target, laser noise is the breadth of the data cloud per laser return (i.e., last, first, etc.). Lower intensity surfaces (roads, rooftops, still/calm water) experience higher laser noise. The laser noise range for this survey was approximately 0.02 meters.

Relative Accuracy
Relative accuracy refers to the internal consistency of the data set - the ability to place a laser point in the same location over multiple flight lines, GPS conditions, and aircraft attitudes. Affected by system attitude offsets, scale, and GPS/IMU drift, internal consistency is measured as the divergence between points from different flight lines within an overlapping area. Divergence is most apparent when flight lines are opposing. When the LiDAR system is well calibrated, the line-to-line divergence is low (<10 cm). See Appendix A for further information on sources of error and operational measures that can be taken to improve relative accuracy.

Relative Accuracy Calibration Methodology

Manual System Calibration: Calibration procedures for each mission require solving geometric relationships that relate measured swath-to-swath deviations to misalignments of system attitude parameters. Corrected scale, pitch, roll and heading offsets were calculated and applied to resolve misalignments. The raw divergence between lines was computed after the manual calibration was completed and reported for each survey area.
Automated Attitude Calibration: All data were tested and calibrated using TerraMatch automated sampling routines. Ground points were classified for each individual flight line and used for line-to-line testing. System misalignment offsets (pitch, roll and heading) and scale were solved for each individual mission and applied to respective mission datasets. The data from each mission were then blended when imported together to form the entire area of interest.
Automated Z Calibration: Ground points per line were used to calculate the vertical divergence between lines caused by vertical GPS drift. Automated Z calibration was the final step employed for relative accuracy calibration.

Absolute Accuracy

The vertical accuracy of LiDAR data is described as the mean and standard deviation (sigma $\sigma$) of divergence of LiDAR point coordinates from RTK ground survey point coordinates. To provide a sense of the model predictive power of the dataset, the root mean square error (RMSE) for vertical accuracy is also provided. These statistics assume the error distributions for x, y, and zs are normally distributed, thus we also consider the skew and kurtosis of distributions when evaluating error statistics.

# Appendix B

LiDAR accuracy error sources and solutions:

| Type of Error | Source | Post Processing Solution |
|---|---|---|
| GPS (Static/Kinematic) | Long Base Lines | None |
| | Poor Satellite Constellation | None |
| | Poor Antenna Visibility | Reduce Visibility Mask |
| Relative Accuracy | Poor System Calibration | Recalibrate IMU and sensor offsets/settings |
| | Inaccurate System | None |
| Laser Noise | Poor Laser Timing | None |
| | Poor Laser Reception | None |
| | Poor Laser Power | None |
| | Irregular Laser Shape | None |

Operational measures taken to improve relative accuracy:
Low Flight Altitude: Terrain following is employed to maintain a constant above ground level (AGL). Laser horizontal errors are a function of flight altitude above ground (i.e., ~ 1/3000$^{th}$ AGL flight altitude).
Focus Laser Power at narrow beam footprint: A laser return must be received by the system above a power threshold to accurately record a measurement. The strength of the laser return is a function of laser emission power, laser footprint, flight altitude and the reflectivity of the target. While surface reflectivity cannot be controlled, laser power can be increased and low flight altitudes can be maintained.
Reduced Scan Angle: Edge-of-scan data can become inaccurate. The scan angle was reduced to a maximum of 315° from nadir, creating a narrow swath width and greatly reducing laser shadows from trees and buildings.
Quality GPS: Flights took place during optimal GPS conditions (e.g., 6 or more satellites and PDOP [Position Dilution of Precision] less than 3.0). Before each flight, the PDOP was determined for the survey day. During all flight times, a dual frequency DGPS base station recording at 1–second epochs was utilized and a maximum baseline length between the aircraft and the control points was less than 19 km (11.5 miles) at all times.
Ground Survey: Ground survey point accuracy (i.e. <1.5 cm RMSE) occurs during optimal PDOP ranges and targets a minimal baseline distance of 4 miles between GPS rover and base. Robust statistics are, in part, a function of sample size (n) and distribution. Ground survey RTK points are distributed to the extent possible throughout multiple flight lines and across the survey area.
50% Side-Lap (100% Overlap): Overlapping areas are optimized for relative accuracy testing. Laser shadowing is minimized to help increase target acquisition from multiple scan angles. Ideally, with a 50% side-lap, the most nadir portion of one flight line coincides with the edge (least nadir) portion of overlapping flight lines. A minimum of 50% side-lap with terrain-followed acquisition prevents data gaps.
Opposing Flight Lines: All overlapping flight lines are opposing. Pitch, roll and heading errors are amplified by a factor of two relative to the adjacent flight line(s), making misalignments easier to detect and resolve.